OXIDATIVE DEHYDROGENATION OF PROPANE TO PROPYLENE OVER $VOx/CaO-\gamma Al_2O_3$ IN A FLUIDIZED BED

BY

AYANDIRAN AFEES AYODEJI

A Thesis Presented to the

DEANSHIP OF GRADUATE STUDIES

KING FAHD UNIVERSITY OF PETROLEUM & MINERALS

DHAHRAN, SAUDI ARABIA

In Partial Fulfillment of the

Requirements for the Degree of

MASTER OF SCIENCE

In

CHEMICAL ENGINEERING

October 2015

KING FAHD UNIVERSITY OF PETROLEUM & MINERALS

DHAHRAN- 31261, SAUDI ARABIA

DEANSHIP OF GRADUATE STUDIES

This thesis, written by **AYANDIRAN AFEES AYODEJI** under the direction his thesis advisor and approved by his thesis committee, has been presented and accepted by the Dean of Graduate Studies, in partial fulfillment of the requirements for the degree of **MASTER OF SCIENCE IN CHEMICAL ENGINEERING.**

B.H.

Dr. Housam Binous
(Advisor)

Dr. Muhammad Ba Shammakh
Department Chairman

Mozhar Hossain

Dr. Mohammad M. Hossain
(Co-Advisor)

Dr. Salam A. Zummo
Dean of Graduate Studies

عمادة الدراسات العليا
DEANSHIP OF GRADUATE STUDIES

Dr. Sameer Al-Ghamdi
(Member)

22/12/15

Date

Shaikh Abdur Razzak

Dr. Shaikh A. Razzak
(Member)

Dr. Muhammad Ba Shammakh
(Member)

This MSc Thesis is dedicated to Almighty Allah, the uncreated creator of all creatures

ACKNOWLEDGMENTS

I wish to acknowledge my sincere gratitude to all those who have rendered their support in various ways in the preparation of these script. First to my advisor (Dr. Housam Binous), co-advisor (Dr. Mohammad M. Hossain), other members of my thesis committee(Dr. Sameer Al-Ghamdi, Dr. Muhammad Ba Shammakh and Dr. Shaikh Abdul Razaq) and all faculties in the Department of Chemical Engineering for their academic and moral support.

I wish to acknowledge King Abdul Aziz City of Science and Technology (KACST) for its financial support.

My sincere appreciation goes to my father, Alhaji Bashiru Ayandiran; my mother, Mrs. Serifah Ayandiran; and my step mother, Mrs. Ruqayyah Ayandiran for their financial and moral support and also for their unique model of guidiance, supervision, exemplary patience and offer of personal assistance with very useful suggestions which have raised the standard of this essay to its present state for which I am most grateful. May God reward them abundantly.

I also give special thanks to my uncle, Mr. Abdulfatai Ayandiran and my elder brother, Mr. AbdulHakeem Ayandiran for their understanding, elderly advice and also their tireless contributions in aid of my research work.

TABLE OF CONTENTS

LIST OF TABLES

LIST OF FIGURES

LIST OF ABBREVIATIONS

ODH:	Oxidative Dehydrogenation
XRD:	X-ray Diffraction
TPD:	Temperature-Programmed Reduction
TPD:	Temperature-Programmed Desorption

ABSTRACT

Full Name : [AYANDIRAN AFEES AYODEJI]

Thesis Title : [Oxidative Dehydrogenation of Propane to Propylene Over VOx/CaO-γAl2O3 in a Fluidized Bed]

Major Field : [Chemical Engineering]

Date of Degree : [October, 2015]

Oxidative dehydrogenation (ODH) of propane is studied with a new vanadium catalyst supported on CaO-γAl_2O_3 under an oxygen free atmosphere. The catalyst is synthesized with different percentage content of CaO (20, 50 and 100 wt %) using vanadyl acetyl acetonate as precursor. The catalyst was proved to be stable over repeated oxidation and reduction cycles via TPR and TPO. NH_3-TPD shows catalyst yield progressive acidity reduction with increase in the wt% of CaO content. TPD kinetics reveals decrease in desorption energy with increase in the level of catalyst acidity. Raman spectroscopy reveals that the catalyst have monovanadate and polyvanadate surface species of VO_x with minute crystal particles of V_2O_5 which is required for good propylene selectivity. FTIR and XRD bands confirms the presence of V_2O_5, CaO and γ- Al_2O_3 in the catalyst. EDXS confirms the elemental composition of the three catalyst. The catalysts were evaluated using CREC Fluidized Bed Riser Simulator at 550-640 ^oC. VOx/CaO-γAl_2O_3 (1:1) catalyst has the highest propane conversion (65 %) and propylene selectivity (85%) and the lowest CO_x due to its moderate level of acidity and intermediate metal-support interactions. Reaction rate as a function of degree of oxidation of catalyst in terms of exponential decay function was used in developing a kinetic model which satisfactorily predicts the propane ODH reaction.

ملخص الرسالة

الاسم الكامل: افيس ايوديجي ايندران

عنوان الرسالة: نزع الهيدروجين بالاكسدة للبروبان الى البروبين باستخدام حفاز $VO_x/CaO-\gamma Al_2O_3$ في جهاز السطح المميع

التخصص: هندسة كيميائيه

تاريخ الدرجة العلمية: أكتوبر 2015

نزع الهيدروجين بالاكسدة للبروبان تتم دراسته باستخدام خفاز جديد لفنيديوم مدعم على $CaO-\gamma Al_2O_3$ تحت جو خالي من الاوكسجين. ويتم اصطناع الحفاز بنسب وزنية مختلفة لاوكسيد الكالسيوم (20, 50 و 100%) باستخدام (فانيدايل أستيل أسيتونات) كمادة بادئة. وقد اثبت الحفاز ثباتيتة بعد اجراء التفاعل عدة مرات عن طريق (TPRو TPO). (NH_3-TPD) اظهر نشاطية حفزية لنقصان الحموضة مع زيادة النسبة الوزنية لمحتوى اوكسيد الكالسيوم. حركية ل (TPD) اظهرت نقصان في طاقة الانحلال بزيادة حمضية الحفاز. مطيافية رامان اظهرت ان الحفاز يمتلك سطح وحيد الفنيديوم و عديد الفنيديوم من نوع (VO_x) و جسيمات بلورية من (V_2O_5) الذي يحتاج انتقائية جيدة للبروبلين. مطيافية الاشعة الحمراء و مطيافية حيود الاشعة السينية اكدتا وجود (V_2O_5, CaO) في الحفاز. مطيافية تشتت الاشعة السينية اكدت التركيب العنصري للحفازات الثلاثة . تم تقيم الحفازات باستخدام (CREC Fluidized Bed Riser Simulator) في درجة حرارة من 550-640 درجة مئوية . حفاز ($VOx/CaO-\gamma Al_2O_3$ (1:1)) اظهر اعلى فعالية لتحويل البروبان بنسبة 65% وانتقائية 85% والاقل هو (CO_x) بسبب حمضيته المعتدلة والتداخلات للفلز المدعوم. معدل التفاعل كدالة لاكسدة الحفاز باستخدام دالة الانحلال الاسي لتطوير نموذج للحركية الذي يتنبأ بتفاعل اكسدة البروبان بصورة مرضية.

CHAPTER 1

INTRODUCTION

1.1 Overview

Propylene is one of the important precursors in the chemical industry to produce different valuable products. Approximately, two third of the propylene produced worldwide is consumed in the production of thermoplastic polypropylene. It is commonly used in fabrication of household appliances, plastic films and many other applications. With increasing world population and improving quality of human life, worldwide propylene demand/sales reaches over ninety billion dollars [1]. Conventionally, propylene has been produced from petroleum refining and olefin cracking processes. In order to meet the ever increasing demand for petroleum fuel and olefins (propylene, ethylene etc), there is a growing need to develop alternative propylene production technology. In this regard propylene from propane, available both in natural gas and refinery off gases, is considered as an attractive technology. The abundant availability of propane in different part of the world including the United States and the Middle Eastern Region, can make these on purpose propylene production even sustainable as compared to the refineries and olefin crackers processes [2].

At present, there are three major commercial processes available in producing propylene, including steam cracking, catalytic cracking (FCC) and catalytic dehydrogenation. Steam cracking process consumes a large amount of heat energy, which accounts for 70 % of the

overall production cost. The coke formation during the cracking of heavy hydrocarbon molecules is the other drawback of the steam cracking process. It causes severe process operational constraints, especially the fouling, which requires frequent plant shut-downs for cleaning. On the contrary, in the FCC process the coke generation is deliberate. The formed coke is combusted in the catalyst regenerator producing heat energy and supplied back to the catalytic cracking unit using the catalyst as energy carrier. This energy is essential for the FCC reactor to carry the endothermic cracking reactions. In FCC process the propylene is obtained as a by products, in addition to the lighter gasoline and other fuels. The yield of propylene can be increased by manipulating the FCC operating conditions and using catalysts additives. Recent research shows that the FCC catalysts can also improve the propylene yield about 4.5 % to 10 %. However, the propylene production cost in FCC process is still high due to the energy requirement by the endothermic cracking reactions. This high energy demand and the continuous catalyst regeneration, make the FCC process capital intensive. Consequently, the building of a FCC for the sole aim of producing propylene is not economical. The third available technology, catalytic dehydrogenation, also suffers from the problem of coke formation and high energy requirement as a result of the endothermic nature of the reaction [3].

1.1.1 Significance of Oxidative Dehydrogenation for Propylene Production

Contrary to the above discussed commercial processes, the oxidative dehydrogenation (ODH) of propane to propylene is more attractive due to its low operational cost and less environmental impacts. Compared to the present commercial technologies, oxidative dehydrogenation reduces costs, save energy and lower greenhouse emissions. The most

important advantage is exothermic nature of the reaction, which requires no additional energy to accelerate the reaction. The formation of water as a by-product of the ODH makes it possible to avoid thermodynamics constraints as observed in the non-oxidative routes. The activity of catalyst is stable for longer cycles because of minimal coke deposition of the catalyst surface [4]. It has been believed that high propylene yield can be obtained through the ODH of propane upon successful development of efficient catalysts. In the ODH process the operation and maintenance costs are low because of the low operating temperature. The use of furnace and the need for decoking shutdowns are also not essential part of the dehydrogenation process. All this counts for comparatively less capital investment and yet provides appreciable operational efficiencies.

1.1.2 The Importance of Fluidized Bed Reactors for Propane ODH

The selection of the reactor is very important for commercial scale application of ODH technology [5]. Fixed bed reactors are simple but difficult to maintain isothermal conditions which can have interference with the performance of the reactor and leads to catalyst damage. There are numerous advantages of fluidized bed reactors over the conventional fixed reactor systems. These include controlled operating conditions at constant temperature, which assist in circumventing the issues with hot spots in fixed bed reactors. Absence of limitations of mass transfer and uniform residence time distributions (RTD) are also merits of fluidized bed reactors. Moreover, transportation of reduced catalytic species from oxidative dehydrogenator to regeneration unit is also one of the merits of fluidized bed reactors that poses periodic catalyst re-oxidation. This enables twin reactors set up, one for oxidative dehydrogenation and other for regeneration of catalyst, which makes it important for commercial scale production [6-8].

1.1.3 Selectivity Control in the ODH of Propane

It was reported in past literatures on oxidative dehydrogenation that vanadium based catalyst gives the highest alkane conversion and alkene selectivity from ethane ODH [9-24]. The wisdom behind this is the provision of lattice oxygen for dehydrogenation of alkanes by vanadium catalyst [25-26].

The reactions involved in the oxidation of propane include the desired propane oxidative dehydrogenation to propylene, combustion of propane and produced propylene to carbon (IV) oxides and carbon (II) oxide. High selectivity for propylene is only feasible at low propane conversions due to lower propane reactivity when compared to propylene. Thus, there is need to design a catalyst that will provide lattice oxygen that will be optimal to the extent that it can selectively produce propylene from ODH of propane without primary and secondary combustion of propane and propylene respectively to carbon oxides [27].

The performance of supported vanadium oxide in ODH reactions is a function of the redox properties and morphology of surface species of VO_x and acid-base character of VO_x catalyst and its support [28-32]. Vanadium catalyst activity and selectivity is a function of the structure of VO_x surface species. The surface density of VO_x increases with vanadium loading, which is lowest for monovanadate isolated VO_x species and highest for monolayer coverage species. Catalyst activity and reducibility increases as surface density of VO_x increases while its selectivity decreases as surface density of VO_x increases [33-37]. Adjustments of the co-ordination and environment of the species of VO_x can influence its catalytic behavior. Acid-base character of VO_x catalyst supports has been explained in past research to have influence on propylene selectivity in ODH [4]. Propane adsorption and

propylene desorption are function of the acid-base properties of the support. Adsorption of basic reactant and desorption of acidic product are function of the acidity of the catalyst. The acidity of the catalyst determines the protection of these chemical species from oxidizing to carbon oxides [38]. The acidic character of alkanes and their corresponding olefins diminishes with increased carbon numbers and degree of molecule saturation; one can hypothesize that higher selectivity in ODH could be achieved by designing catalysts with controlled acidic character [39-40].

There are usually strong interactions between the support (carrier) and the active site (VO_x). Gamma aluminum oxide is not inert towards VO_x. Its interaction towards VO_x phase is not weak, hence it result in a very high dispersion of V_2O_5 on its surface. High vanadium loading can be achieved on γAl_2O_3, but resulting samples will show lower surface areas unlike CaO which has higher surface area. The use of CaO will improve resulting catalyst's superficial area and also gives it the desired moderate level of acidity, that will maximize propane adsorption and propylene desorption and also minimize propylene and propane combustion. Hence, the synthesis of mixed γAl_2O_3/CaO supports is an interesting route to achieve catalyst samples with high dispersion of the surface active species, and a surface area that is higher than that of γAl_2O_3 [41].

1.1.4. Contribution of the Work

After all necessary contributions, the present work was focused on investigating VOx/CaO-γAl_2O_3 catalyst for ODH of propane to propylene and the following contributions were made:

(i) Novel VOx/CaO-γAl_2O_3 catalysts with different compositions of CaO that give good propane conversion and propylene selectivity was developed

(ii) A kinetic model that fit the experimental data obtain from the propane ODH experiment was developed

CHAPTER 2

LITERATURE REVIEW

2.1 Overview

This work focuses on oxidative dehydrogenation of propane to propylene in a Fluidized Bed. Therefore; an overview and theoretical information pertaining different types of dehydrogenation processes, oxidative dehydrogenation reactors, oxidative dehydrogenation catalysts including vanadium is presented in this chapter.

2.2 Dehydrogenation Processes for Propylene Production

Propylene is an essential chemical precursor. It can be used to produce polymers. It is largely utilized to yield polypropylene, which represent about sixty seven percent of the universal demand. Polypropylene finds application in the automobile, electrical, packaging and plastic films industries. Apart from polypropylene production, propylene is also used in producing acrylonitrile and propylene oxide. Propylene demand is rising, hence its synthesis has a pronounced marketable importance. One of the most vital method of synthesizing propylene as a byproduct is the steam cracking of oil gas, naphtha or alkanes. A substantial amount of energy is requisite for this process. Fluid catalytic cracking (FCC) can also be used to produce propylene. The key purpose of FCC units is to synthesize gasoline, propylene is also obtain here as a by-product just like the case of steam cracking

process. Propylene is not the most essential product for FCC units, and thus it is usually accompanied with bad yield. A lot of research is currently carried out to maximize the yield of propylene from FCC units due to the rise in the demand for propylene [42]. Lastly, there is a possibility of synthesizing propylene through the process of catalytic dehydrogenation of propane, as shown in the following reaction:

$$C_3H_8 \rightarrow C_3H_6 + H_2 \quad (2.1)$$

However, this reaction is strongly endothermic with enthalpy of 124000 Joules per mol which makes it to necessitate 873 K reaction temperature, thus the reaction is not easy to carry out. Since the early twentieth century, researchers have been utilizing noble metals as catalyst for the dehydrogenation of alkane. Specifically, Platinum based catalysts can be utilized in the dehydrogenation of propane, due to their high catalyst activity. At present, propane dehydrogenation can be carried out via numerous catalytic processes. Certainly, an orthodox propane catalytic dehydrogenation is well-known and utilized in industries across the globe. However, all the existing processes agonize from countless numbers of challenges. The most essential of the challenges is that the rapid deactivation of catalyst, as a result of formation of coke. Therefore, a high active catalyst that will not deactivate rapidly is required. Besides, an external source of heating is required because of the endothermic nature of the reaction. At the moment, the universal energy demand is on the increase, and generally they have limited sources, which include the fossil energies [42]. The cost of energy is rising. Therefore, to get a process utilizing a smaller amount of energy is a major challenge. Some catalysts have great potential in carrying out this reaction. The mechanisms of the catalytic reaction are not well-known. The all-purpose principle for catalytic reaction mechanisms was not found, only a small number of the mechanisms were

elucidated by scientists. Why some catalysts are very active for a particular reactant and not active with other reactants remains a question that is yet to be answered by researchers. Therefore, an efficient catalyst for the propane dehydrogenation is difficult to discover, and finding a novel technique to synthesis propylene remains a challenge. The comparison of dissimilar catalysts in propane dehydrogenation is a very fascinating analysis. The outcome of the reaction is a function of different constraints. Optimization of the numerous constraints, which include the internal pressure of the reactor, constituents of the feed, temperature, is a time-consuming but inspiring research. There is a new technique that is being currently studied for propylene production. The technique is refers to as the oxidative catalytic dehydrogenation of propane.

The catalytic dehydrogenation of propane can be done in five ways, namely non-oxidative dehydrogenation, oxidative dehydrogenation, Authothermal dehydrogenation and Selective Combustion Dehydrogenation.

2.2.1 Non-Oxidative Dehyrogenation

A non-oxidative dehydrogenation of propane is a famous technology. Here, the feed gas consists of propane, hydrogen and an inert gas. UOP Oleflex, ABB/Catofin, Snamprogetti, Phillips STAR, PDH (Linde) are some of the processes used for the reaction. For instance, the PHD (Propane DeHydrogenation process) by Linde-BASF-Statoil, is centered on a steamreformer form of dehydrogenation reactor. The reaction section comprises of three reactors. Two of them involves dehydrogenation, while the third reactor deals with catalyst regeneration combustion of coke in a mixture of steam-air. The foremost benefit of the

process, as compared to other processes, is the non-existence of reactant dilution. This permits to diminish the dimensions of the reactor, and to make the product's purification easier. The temperature of the reaction is regulated very carefully in this case [42].

However, these processes are accompanied with a lot of difficulties. The amount of heat required for the reaction to take place is very high which leads to its high cost which is one of the difficulties encountered in the process. Therefore, as the demand for propene is growing, novel technologies need to be established to enhance propane dehydrogenation.

2.2.2 Oxidative Dehyrogenation (ODH)

Production of propylene is possible by utilize oxygen in the course of the dehydrogenation reaction. Here, an oxidative dehydrogenation occurs in accordance with the following equation:

$$C_3H_8 + ½\ O_2 \rightarrow C_3H_6 + H_2O \qquad (2.2)$$

This reaction is highly exothermic, so it is an interesting alternative to simple dehydrogenation. This reaction is a good alternative to non-oxidative dehydrogenation because it is exothermic. The challenge associated with this reaction is the parallel reaction to the unrequired combustion of alkane. For instance, there might be complete combustion of propane which will yield carbon(IV)oxide or incomplete combustion of propane which will yield carbon(II)oxide. There could also be complete and incomplete combustion of the produced propylene to yield carbon(IV)oxide and carbon(II)oxide respectively. This will have effect on the selectivity of propylene. Excess heat must be taken away from the

reaction since it is highly exothermic. This can be achieved using heat exchangers. A. Propane oxidative dehydrogenation was studied using an Alumina supported Platinum catalyst (Beretta *et al.*) using an annular reactor. This was done by loading a catalyst of small quantity in the reactor. A well-controlled temperature and high space velocity was achieved. They observed that there is high catalyst activity at all the temperatures. Besides, they compared this kind of dehydrogenation at high temperature with or without catalyst. The products and their quantities were compared with or without catalyst. It was observed that propane ODH can only take place at low and medium temperature when catalyst is used. They were no significant different in terms of product formed and its quantity between using or not the catalyst at high temperature. These lead to their conclusion that reactions in gas-phase will have high activity and selectivity in producing alkenes at high temperature [43].

2.2.3 Autothermal Dehyrogenation (ADH)

During normal dehydrogenation, an external heat supply is required. Unlike the case of normal dehydrogenation in which an external supply of heat is needed, autothermal dehydrogenation process is free from this challenge. Here, the dehydrogenation of alkane is accomplished by utilizing a combination reaction of hydrogen. Oxygen from gaseous feed reacts with hydrogen to produce water. At typical dehydrogenation conditions, The combustion of half of the formed hydrogen provides necessary heat which as compensation for the endothermic loss phenomenon of the reaction.

2.2.4 Selective Combustion of Hydrogen (SCH)

A Selective Combustion of Hydrogen was also studied by some equips. Here, part of the hydrogen produced in situ was made to undergo combustion in order to furnish the required heat of reaction. Hydrogen gas burning is expected to shift the equilibrium of the dehydrogenation reaction towards products. Another benefit of this process is that catalyst coking can be reduced with oxygen gas or steam atmosphere. Combination of a Selective Combustion of Hydrogen unit and traditional unit of propane dehydrogenation is possible.

2.2.5 Non-catalytic Oxidation Dehydrogenation

This is another type of oxidative dehydrogenation reaction, but it is carried out without the catalyst. Without the use of catalyst, it will have less selectivity and yield of propylene and higher yield of carbon (IV) oxide and carbon (II) oxide when compared to the catalytic oxidative dehydrogenation reaction.

2.3 Oxidative Dehydrogenation Reactors

Oxidative dehydrogenation of propane is still not a commercial process, but a lot of research has been carried out on it using different reactors. In 2001, Raquel Ramos et al worked on this process using V/MgO as catalyst. They used a tubular reactor that has a specification of six millimeters internal diameter and made from quartz. It was placed in an electric furnace which is at 1 atm [44] A similar reactor was used in 2007 using V_2O_5/

Al_2O_3 and MoO_5/Al_2O_3 Catalysts using a reactor that was placed in a tubular furnace, which is meant to increase the temperature of the system [45]. Changlin Yu et al; in 2007 also worked on this process using a fixed bed reactor made from quartz using a platinum catalyst that was doped with Zinc. Yu Chang-lin et al; 2007 used a catalyst of PtZn-Sn/SBA-15 catalyst in a fixed bed reactor made from quartz [45] Ejiro Gbenedio et al 2007; utilizes a Paladium/Alumina in membrane reactor, which is also a fixed bed reactor and it was made from hollow fibre" [46]. In all these experiment, the reactor used was made from quartz, which is the second most abundant mineral in the Earth continental crust after feldspar. It has silicon–oxygen tetrahedra in a way that each oxygen is being shared between two tetrahedra between with each O_2 being shared between two tetrahedra, which gives SiO_2. It has a specific gravity of about 2.65 and refractive index of 1.543–1.545. It has a melting of about 1700 ^{0}C and is insoluble at standard temperature and pressure (STP).

Some authors also worked on propane dehydrogenation using similar reactor but made from stainless steel rather than quartz. For instance, In 2012, Baba Y. Jibril et al; worked on the performance of supported $Mg_{0.15}V_2\ O_{5.15}\ 2.4H_2O$ nanowires using a stainless steel tubular reactor made from an alloy known as stainless steel which has a specification of 0.305m long and internal diameter of 0.009m [47]. During the same year 2012, Yongzheng Duan et al used a stainless fixed-bed tubular reactor under 863K at 1 atm [48]. These types of reactors are different from the previously discussed ones due to the use of stainless steel. Generally stainless has a density of about 8g/cm^3, Young's modulus of about 200,000, thermal expansion of about $13 \times 10^{-16}/^0$C, thermal conductivity of about 20 W/m ^{0}C, heat capacity of 400 J/Kg ^{0}C, and resistivity of about 700 nΩm at 20 ^{0}C. Although stainless steel is robust, leak-tight, can withstand high pressure but it cannot without high

temperature. Materials made from Quartz are transparent, inert, can withstand high temperature and can only withstand low pressure like the atmospheric pressure that is employed in the oxidative dehydrogenation process. From these stated properties, reactor made of quartz are more preferred for oxidative dehydrogenation because it can withstand high temperature and show inertness properties [49].

A special micro-structured reactor came into limelight recently. In 2012, Mengwei Xue et al; worked on propane oxidative dehydrogenation using a material using a tubular micro-reactor that is conventional and made from quartz [50]. A similar reactor was used in 2013 by Guangjun Wu et al; who worked with nitrous oxide over Fe-ZSM-5 prepared by grafting: and Yiwei Zhang et al who worked with Al_2O_3 catalyst that employed PtSnNa/La as a dopant [51]. The conventional quartz tubular micro-reactor was more recent in comparison to the reactor with a fixed bed. In a fixed bed reactor for propane ODH, inspite of catalyst dilution, temperature changes occur upon increasing reaction temperature and reactant concentration in the feed. In the micro-reactor, no temperature gradients were observed under all applied conditions. Therefore, the micro-reactor offers a good temperature control and can be applied for studying reaction kinetics of a strongly exothermic reaction as the oxidative dehydrogenation of propane under isothermal conditions within a wide range of reaction conditions.

Al-Ghamdi in 2013 worked on a Ph.d desertation titled “Oxygen-Free Propane Oxidative dehydrogenation over vanadium oxide catalysts: reactivity and kinetic modeling” He used a reactor known as CREC Riser Stimulator. This was invented by Professor Hugo de Lasa at the department of Engineering in University of Western Ontario. It allows new catalysts to be developed and has led to the launch of Reactor Engineering and Catalytic

Technologies. The CREC Riser Simulator is a batch reactor is similar to the continuous 'riser' and 'downer' units used in the industry. Traditional bench or large scale units don't accurately reproduce industrial reactor conditions, leading to inaccurate catalyst test results in terms of conversion of feedstock and selectivity of product. They have expensive mode of operation are constraint to specific processes, making it difficult to test a wide range of catalysts. Western's Riser Simulator permits the research and development of new processes including oxidative dehydrogenation. The CREC Riser Simulator allows new catalysts to be investigated at less than one-tenth the cost of units of pilot plant. Operating costs are minimized, since testing only requires small amounts of catalyst and reactant and a single operator. By using such small quantities, the Simulator's unique design makes it suitable for catalyst evaluation and development while significantly simplifying the experimental procedure and related catalyst synthesis. The Riser Simulator is very good for large scale catalytic reactor simulation, catalyst characterization and kinetic modeling. Multiple runs allow new catalysts to be characterized quickly and efficiently and the Simulator's unique design allows for instantaneous feeding of reactant and removal of product. The Riser Simulator is able to duplicate any operating condition that is desired accurately, and it can be used to explore different operating parameters such as temperature, pressure, contact time or catalyst loading, all of which are required for true evaluation of catalyst and kinetic modeling. Ultimately, the Riser Simulator can assist companies adhere to more stringent environmental guidelines.

The Riser Simulator is an innovative unit developed to solve the technical problems of micro activity test units which can be applied for vast functions ranging which include evaluation of industrial catalysts at commercial conditions, carrying out kinetic and

modeling studies for some specific reactions. It can be used for a wide range of reaction time and temperature and broad range of total pressures. It can also be used for different feedstocks including propane. It also provides a very easy means of catalyst regeneration. A small quantity of feed and catalyst is required when working on evaluation of catalyst using a riser simulator. All these qualities make the CREC Riser Simulator to be very suitable for propane ODH.

2.4 Oxidative Dehydrogenation Catalysts

Metal oxides together with additives or without the additives which include alkali metals and halides, supported on metal oxide supports such as MgO, SiO_2, CeO_2, Al_2O_3, ZrO_2, TiO_2, and zeolites has continued to be a point of focus for the development of catalyst for ODH reactions. It has also been reported to have great influence on the selectivity and activity of the ODH catalyst. Indeed, the following reasons make it quite difficult to have a uniform picture regarding those important catalyst features that define the performance in alkane ODH [52].

1. A meaningful percentage of research works emphasis on certain definite aspects that may have effect on the reactivity of the catalysts examined. A good illustration of this is the instance of supported metal oxide catalysts, in addition to the usual morphological aspects, a number of the significant features that has effect on the performance are: acid–base characteristics; the metal cation valency state under conditions of reaction; the degree of agglomeration of these metal cations; the combined electronic properties of the solid.

Each of the above-mentioned aspects is important as revealed from experimental facts, and one may occasionally have the impression that the significant factor may be any one of them, depending on what the investigator is looking for. It is glaring that what is missing is an interpretation that is collective and would have the capability of bringing all these aspects together and outlining a general picture.

2. Apparently, the conflicting report deduced from dissimilar conditions of experiment, not so much with regards to the steps utilized for synthesis of catalyst and thermal treatment, as the catalytic tests condition. The condition for catalytic test may vary greatly. The reaction temperature, pressure, contact time, the feed ratio between oxygen and alkane are key operative parameters. Oxygen-lean conditions are often used, in order to obtain better selectivity to the olefin; which implies that the total conversion of O_2 is reached and that, depending on the temperature, reactions leading to the formation of H_2 may become significant. Therefore, the redox properties of the gas phase (either reducing or oxidizing) with regard to the metal cations are influenced by these operative parameters [53].

2.5 Supported Vanadium Oxide Catalyst

A lot of research has been carried out on the possible application of vanadium-based catalyst. This works show that it has very high activity and selectivity for propane ODH. The reason behind this is the provision of lattice oxygen for the elimination of hydrogen from propane. It involves the reduction of vanadium oxide to yield reduced vanadium cations when its lattice oxygen part interact with propane. The cation later interact with gas phase molecular O_2 to form air to reproduce the vanadium oxide. [33]

$$C_3H_8 + VO_X \longrightarrow C_3H_6 + H_2O + VO_{x-1} \quad (2.3)$$

$$VO_{x-1} + ½\ O_2 \longrightarrow VO_x \quad (2.4)$$

There are basically two significant factors in ODH reactions that is influenced by the behavior of vanadium oxide catalyst. They are the acid-base character of the dual function catalyst and the redox properties and structure of the surface species of VO_x. These factors are function of the loading of vanadium and the type of the support. It was established that V_2O_5 catalyst supported on TiO_2 is the more active catalyst for propane ODH and V_2O_5 catalyst supported on Al_2O_5 is the more selective catalyst for propane ODH. However metals like molybdenum, zinc, potassium, calcium, magnesium, gold, nickel, chromium, phosphorus e.t.c can serve as additive for the ODH reaction catalyst. They served as dopants. They are used basically to improve the catalyst acidic and basic properties. The selectivity of propylene in ODH of propane can be improved on by addition of alkali and/or alkaline earth metals [46].

2.6 Production of Vanadium Oxide Catalysts

It is of no doubt that the pillars of industrial chemical transformations are catalysts. Of the products made from chemical industry, approximately 85%-90% are synthesized via catalysis [11]. The particles' size and shape, the volume and size of pore, and the area of the surface are the vital physical properties of the catalyst and its support. Transition metals and their compounds function as catalysts for different reactions due to their capacity to modify oxidation state, to serve as adsorbent for other substances on to their surface and

activate them in the process. However, due to the chemical and physical properties of vanadium, it is thought to be one of the greatest essential and beneficial metals to be utilized as a catalyst. It is of no doubt that vanadium represents the most dominant non-metallurgical use in the field of catalysis. Vanadium oxide catalysts have wide applications in numerous industrialized processes of catalysis, resulting into beneficial yields [2, 50, 54, 55] and, in various catalytic reactions with a pilot scale, are coming up to be enhanced so they can at the end be useful at industrial scale [48, 56-58]. In countless instances, selectivity or activity could be expanded by doping with developers, whereas dissimilar supports are utilized to increase their mechanical strength, durability and ability to withstand heat. There have been lots of published research papers on oxidation catalysts which contains vanadium. Vanadia's catalytic activity is credited to its capacity to simply modify its state of oxidation of 3 to 4 or 5, and its nature of reducibility [59]. Majority of the catalysts that are grounded on VOx comprises of deposit of phases of vanadia on the oxide support surface, which include Silicon (IV) oxide, Aluminium (III) oxide, Titanium (IV) oxide, Zirconium(IV), and in small amounts on Cesium(II)Oxide, NbO5, Magnesium Oxide and zeolites. Vanadium oxide introduction approach onto a support has an important effect on the properties of the active site of the catalyst. Normally, the foremost technique of diffusing VOx on the above-mentioned support materials is the standard insipient-wetness impregnation technique. Also, adsorption from ion exchange techniques and also from the solution (grafting) have also been utilized comprehensively. Other techniques of catalyst preparation have been utilized to a lesser degree, which include [60], pyrolysis of flame spray [61, 62] and vapour-fed flame preparation. The process of depositing chemical vapor using volatile molecular metal precursors to modify the surface of the support oxide

and make available a technique to control the active sites dispersion have also been utilized. The impregnation technique is usually utilized to prepare VOx catalysts for oxidative dehydrogenation of propylene. It signifies a process in which a definite volume of solution which contains precursor of VOx is placed in contact with the solid support. If the pore volume of the support is the same or greater than the volume of solution, the method is incipient wetness [53]. This actual preparation method, as proved from past research works, shows a wide disparity of species of VOx surface at loadings that is less than the coverage of the monolayer, depending on the conditions of preparation. Besides, it gives slight control over surface species and their dispersion. It may also lead to the development of V_2O_5 that has three dimension, even at minute loadings of vanadium oxide [41]. Impregnation of dissimilar supports, such as organic soluble precursors such as solutions of either vanadyl acetyl acetonate in toluene or propanol, have revealed that a greater quantity of VOx can be mixed with the support material, yielding a catalysts that has high dispersion without nanoparticles of vanadium (V) oxide of three dimension that is lower than the loading required to produce the monolayer. Grafting methods have been extensively utilized to synthesis supported catalysts [46, 48, 49]. The technique assists in achieving a great fraction of loading of metal and as well aids to scatter the sites of active metal by suitably changing the synthesis techniques. The method of ion exchange licenses that ionic species of vanadium oxide existing in an aqueous solution are attracted by charged sites of the support surface through electrostatics.

It is imperative to lay emphasis on the fact that besides the techniques utilized to scatter VOx on dissimilar material supports, the process of calcination used to synthesize the VOx catalyst is also essential to consider for producing the favorite constituent of active catalyst.

At elevated temperatures calcination, there can be formation of compounds of mixed oxide or solid solutions with a number of oxide supports. Furthermore, it is significant to mention that the majority of the aforementioned techniques, except for the FSP technique, are intrinsically limited in scalability. Majority of them have been utilized to synthesis minor catalyst quantities, largely as model catalysts. Although they have revealed reproducibility to some degree, batch effects cannot be omitted entirely.

Summarily, the relative concentrations of the species of surface vanadia powerfully influences the particular metal oxide support, the density of surface vanadium , the catalyst preparation technique, the condition of synthesis, solvents, and the temperature of calcination. Indisputably, new intuition into the synthesis of supported VOx catalysts is anticipated in the near future. Certainly, the preparation and molecular design of highly productive catalysts need changing ideas of solution chemistry, solid-state chemistry, and inorganic chemistry in addition to good experimentalist skills, which altogether will deliver the optimal tactic to synthesis catalysts by design.

2.7 Performance of Catalyst for Propane ODH

Table 2.1 Comparison of the Performance of Some Catalysts for Propane ODH to produce Propylene

S/No	Catalyst	T(^{0}C)	C_3H_8 conversion	C_3H_6 Selectivity(%)	References
1	Al-C	450	9.4	51	De Leon et al, 2014
2	Al-Cr-C	450	26.7	62	De Leon et al, 2014
3	Cr-C	450	26.3	36	De Leon et al, 2014
4	PtSnNa/Li-Al	590	41.1	96.2	Yiwei Z et al, 2013
5	Pt/H-Beta	540	45.5	30.8	Yiwei Z et al, 2013
6	Pt/Na-Beta	540	30.5	35.7	Yiwei Z et al, 2013

7	Pt/Na-ZSM-5	555	44.8	55.4	Yiwei Z et al, 2013
8	PtZn/Na-Y	555	24.8	91.6	Yiwei Z et al, 2013
9	PtSnK/ZSM-5	590	33.8	91.4	Yiwei Z et al, 2013
10	PtSnNaLa/ZSM	590	41.5	97.1	Yiwei Z et al, 2013
11	PtSnNa/Al SBA-	590	27.5	94.1	Yiwei Z et al, 2013
12	PtSnCa/ZSM-5	590	34.9	51.4	Yiwei Z et al, 2013
13	FeMFI-24G-1073	475	46.3	64.8	Guangjun et al, 2013
14	FeMFI-24LE-1073	450	26.7	69.1	Guangjun et al, 2013
15	FeMFI-24SE-1073	475	51.6	23.9	Guangjun et al, 2013

16	FeMFI-24IS-1073	450	46.7	50.2	Guangjun et al, 2013
17	FeMFI-24IS-873	450	43.3	50.6	Guangjunet al,2013
18	$PtSn/Al_2O_3$	580	20.86	93.59	Li J et al; 2013
19	$PtSn/Al_2O_3$	650	36.33	83.98	Li J et al; 2013
20	$Pt@SnO_2$/Al2O3	580	23.82	98.52	Li J et al; 2013
21	$Pt@SnO_2$/Al2O3	650	41.49	92.98	Li J et al; 2013
22	Pt-Sn/Al-SAPO34	590	40	95	Zeeshan, 2011
23	Mg/MgMoOx	450	1.8	78.9	Koc et al 2004
24	Ni(15)/MgMoOx	450	3.1	81.9	Koc et al 2004
25	Yi(10)/MgMoOx	450	3.1	99.5	Koc et al 2004
26	La/MgMoOx	450	1.7	96.7	Koc et al 2004

27	VAl_2O_3	452	13.7	49.7	Lemonidou et al 2000
28	VAl_2O_3	500	13.8	28.8	Lemonidou et al
29	$LiVAl_2O_3$	452	7.5	73.7	Lemonidou et al 2000
30	$LiVAl_2O_3$	500	23.9	49.6	Lemonidou et al 2000
31	$NaVAl_2O_3$	452	6.2	77.3	Lemonidou et al 2000
32	$NaVAl_2O_3$	500	20.2	50.7	Lemonidou et al 2000
33	$KVAl_2O_3$	452	5.7	80.2	Lemonidou et al 2000
34	$KVAl_2O_3$	500	16.9	57.2	Lemonidou et al 2000

CHAPTER 3

OBJECTIVES

Based on the numerous details explained in the introduction and the literature review the objective of this MSc research is to give a profound study on a new CaO/Al_2O_3 mixed supported-vanadium ODH catalyst. This include the reactivity of this ODH catalyst and its stability. Another objective of this work is to achieve this research in an atmosphere that is free of oxygen using a particular fluidized bed reactor that is known as the CREC Riser Simulator. In order to accomplish this, the precise planned objectives for this MSc research are highlighted below:

(i) The synthesis of new $VOx/\gamma\text{-}Al_2O_3/CaO$ catalyst that can be fluidized. Variation of $\gamma\text{-}Al_2O_3/CaO$ content for propane ODH with constant 10% weight of VOx was used in order to arrive at five different samples.

(ii) The characterization of the $VOx/\gamma\text{-}Al_2O_3/CaO$ catalyst samples with dissimilar surface characterization methods such as, Hydrogen gas- Temperature-Programmed Reduction, Scanning Electron Microscope Analysis, X-ray Diffraction, Fourier Transform Infra Red Spectroscopy, Ammonia-Temperature-Programmed Desorption and Laser Raman Spectroscopy,

(iii) The development of different runs of reactions to launch several performances of $VOx/\ \gamma\text{-}Al_2O_3/CaO$ catalyst for oxidative dehydrogenation of propane in a CREC Riser Simulator by utilizing fluidized bed reaction conditions. The different runs

was established to study how oxidative dehydrogenation reaction is a function of contact time and temperature of reaction.

(iv) Development of Kinetic Modelling that fits in the experimental data obtained from the ODH reaction runs and evaluation of kinetic parameters

CHAPTER 4

EXPERIMENTALS

4.1 Introduction

This chapter explains the methods and methodology convoluted in the synthesis, the characterization and the evaluation of the Vanadium Oxide Supported on Al/Ca Mixed Oxide catalysts (VOx/ γ-Al_2O_3/CaO) for oxidative dehydrogenation (ODH) of propane. The first segment of this chapter reports the processes followed in the synthesis of the catalyst and the dissimilar methods used to characterize this catalyst samples. The concept and experimental techniques of various characterization methods used are concisely explained. Wherever possible, the current status about characterization technique applications for catalysts containing vanadium is also briefly reviewed. The second segment of this chapter provides a detailed description for the CREC (Chemical Reactor Engineering Center) Riser Reactor Simulator Unit used for establishing the activity of the prepared catalyst samples under fluidized bed reactor conditions.

4.2 Catalyst Synthesis

The catalyst samples were prepared by impregnation method through soaking with excess ethanol as solvent. Before metal loading, the γAl_2O_3 and CaO supports were calcined under pure N_2 flow at 500 ^oC for 4 hours, to remove moisture and volatile compounds. The

calcined γAl_2O_3 sample was placed in a beaker and ethanol was added. Desired amount of vanadyl acetyl acetonate and CaO were then added to the beaker, and the mixture was left under stirring for 12 hrs. The mixture was then placed for sonication for 10 mins. The mixture was filtered and dried in the atmospheric conditions evaporating ethanol. Following the nature evaporation, the sample was placed in an oven at 100 ^{o}C for 24 hours in order to slowly remove any remaining solvent. The dried sample was then reduced with hydrogen (10% H_2 and 90% Ar) at 500 ^{o}C in an especially designed fluidized bed reactor. Finally, the reduced sample was calcined under air at 500 ^{o}C for 4h to obtain the oxide for of the catalyst. After this treatment, catalyst color became yellow indicating the presence of V_2O_5 on the support surface.

Following the above approach, two catalysts samples were prepared with CaO to γAl_2O_3 weight ratios of 1:4 and 1:1, respectively while keeping same 10 wt% vanadium loading (VO_x/CaO-γAl_2O_3(1:4), VO_x/CaO-γAl_2O_3(1:1)). The third sample was prepared using pure CaO as support and 10 wt% vanadium (VO_x/CaO).

4.3 Catalyst Characterization

4.3.1 SEM-EDXS analyses

The elemental analysis of the prepared sample were conducted using energy-dispersive X-ray spectroscopy. For analysis, the catalyst samples were dispersed on a stub that is tapped with copper. Each of the samples were coated with gold in order to eliminate charge build-up, obtain better contrast and enhance visibility at magnification of one million times. The

sample was analyzed by the SEM, while ensuring that the microscope is aligned in order to avoid lack of sharpness and focus. An electron beam is incident across the catalyst sample resulting in the generation of secondary and back scattered electrons, which are used to form images and X rays which was used to obtain elemental constitution of the catalyst samples.

4.3.2 X-ray diffraction (XRD)

The crystallographic structure of the catalyst samples and the bare supports were investigated using X-ray diffraction analysis. The XRD patterns of all the samples were noted with monochromatic Cu Kα radiation of 1.5406 $\times 10^{-1}$ nm wavelength, 50 mA electrical current, 10 kV electrical voltage and 2^{o} scan per minute (normal scan rate) within 2θ range from 10^{o}-90^{o} with 0.02 step size on a Rigaku Miniflex diffractometer.

4.3.3 Laser Raman Spectroscopy

The molecular structures of various metal oxide species supported on CaO-γAl_2O_3 and CaO were analyzed using a Horiba Raman spectrometer attached to a confocal microscope. For each experiment, 0.5 g of sample was dehydrated under dry air for an hour at 500 ^{o}C and then cooled to ambient temperature with a thermoelectrically cooled CCD detector (-73^{o}C) equipped with the Raman spectrometer. An argon ion laser line of 532 nm wavelength was used to excite the catalyst samples. The Raman spectrometer was used for

measuring and recording the spectra produced from the excitation with a resolution of one cm^{-1} at room temperature.

4.3.4 FTIR Spectroscopy

Nicolet 6700 Thermo Fischer Scientific instrument recorded the FTIR spectroscopy of the synthesized catalyst samples and the bare support γAl_2O_3 and CaO samples. For analysis, 3 mg of sample was uniformly mixed with 0.4 g of potassium bromide. The infrared spectra of pelletized samples were later collected in the range of 400-4000 cm^{-1}.

4.3.5 Temperature Programmed Reduction (TPR)

The reduction temperature and the reducibility of the sample were determined using temperature programmed reduction technique. A Micrometrics AutoChem II 2920 analyzer was used to conduct H_2-TPR experiments at 101.3 KPa. For TPR analysis, 0.05 g catalyst sample was loaded in a U-shaped quartz tube using glass wool to hold the catalyst particles inside. The tube was inserted into retaining nuts and O-rings and then positioned in a tube ports placed in a heater. Before analysis the sample was pretreated under Ar flow at 500 ^oC to remove any volatile component. After pretreatment, the sample was completely oxidized by circulating a gas mixture of 5 % O_2 and balanced He, at 500 ^oC with a heating rate of 10 ^oC/min. The sample was then cooled down to ambient temperature under Argon flow to ensure flushing out any gas phase O_2 that might have trapped in the catalyst bed. The temperature programmed reduction experiment was carried out by circulating a gas stream of 10 % H_2/Ar at 50 cm^3/min. At this conditions the sample

temperature was raised from the room temperature to 850 °C at a heating rate of 10 ^{o}C/min. With the increasing the bed temperature, hydrogen started reacting with the solid phase metal oxides producing water vapor. This water vapor was trapped by circulating the exit stream through a clod trap containing molecular sieve. The water free outlet gas stream was passed through a calibrated thermal conductivity detector (TCD) which detects the variation of the hydrogen concentration due to the reduction of the catalyst samples.

4.3.6 Temperature Programmed Desorption (TPD)

The acidity and acid strength of the catalyst were investigated using ammonia the temperature programmed desorption analysis. The NH_3-TPD desorption kinetics analysis also helps evaluating the metal–support interactions of the supported catalyst. In the context of the present study, the NH_3-TPD experiments were conducted using an AutoChem II 2029 Analyzer received from Micromeritics, USA. Similar to the TPR experiments, 0.05 was first loaded into the U-shaped quartz container and degassed for 2 hrs at 500 ^{o}C under Ar flow at 30 ml/min. The sample was then cooled to 120 ^{o}C and brought to saturation with ammonia using a NH_3/He gas mixture (5% NH_3/He) at a rate of 50 ml/min. Following the ammonia saturation, the system was purged with helium at 100 ^{o}C at 50 cm^3/ min to remove any gas phase ammonia in the system and unadsorbed ammonia trapped in the catalyst bed. For desorption analysis, the catalyst bed temperature was raised from room temperature to 750 °C at 10 ^{o}C/min. The ammonia chemisorbed was desorbed as the temperature elevated to 750 ^{o}C. The ammonia concentration of the effluent gas was monitored by the thermal conductivity detector.

4.4 Fluidized ODH of propane evaluations

The gas phase oxygen free ODH propane experiments were conducted in a fluidized CREC Riser Simulator (CREC: Chemical Reactor Engineering Centre). The CREC Riser Simulator, a bench scale fluidized reactor (53 cm^3), is very useful for catalyst evaluation and kinetic studies. It has outstanding advantages including simulating fluidized conditions of a riser/downer reactor even with a small amount of catalyst, minimize mass transfer limitations by using small sized catalyst particles, constant residence time distributions and controlled isothermal conditions. The CREC Riser Simulator reactor operates alongside with different accessories which include temperature controllers, gas chromatography, vacuum box, main power switch, water pressure indicator and push button selector. The details of the CREC Riser Simulator can be found in Al-Ghamdi et al. 2012 [6].

Propane ODH runs were carried out at different temperature ranging from 550 °C to 640 °C while reaction time was varied between 10-31 sec. The reaction temperatures were selected within the reduction temperature range of the catalysts as determined by TPR study, given the solid catalysts is the only source of oxygen. The ODH of propane experiments were conducted using 0.5 g of catalyst. The oxidized catalyst sample was loaded into the catalyst basket located in the lower shell of the main reactor body of the CREC Riser Simulator. Following the catalyst loading, the system was pressurized up to 30 psi at room temperature to perform leak test. A stable pressure reading at closed condition confirmed absence of any leak. Now the reactor is ready to be heated to the desired temperature. During the heating period, the system was maintained under argon flow to keep the reactor from any air interference. Once the reactor reached to the desired

temperature level, the argon flow was stopped. Consequently, the reactor pressure started to decrease sharply. The four port valve was closed, as the reactor pressure approached to one atm (14.7 psi). Following the isolation of the reactor, the vacuum pump turned on to evacuate the vacuum box down to 20.7 kPa (3.75 psi). A preloaded syringe was used to inject 1.2 ml of feed (propane) into the reactor after setting the impeller on motion. The pressure transducer was used to record the pressure profile of the reactor. The analysis of the product was carried out with the aid of an online GC equipped with three different packed columns. Two of them are the carbon-1000 and carbon-1004 columns which were used for separating the hydrogen, oxygen, nitrogen, argon, carbon (IV) oxide, carbon (II) oxide gas and they were serially connected with the thermal conductivity detector (TCD). Flame Ionization Detector (FID) was utilized in detecting the hydrocarbons which propane, propylene, ethane, ethylene and methane after they were separated with the Haye SepD column. Catalyst performance was studied based on propane conversion, selectivity and yield given below.

$$\text{Propane conversion, } X_{C_3H_8}(\%) = \frac{\sum_j z_j n_j}{3n_{propane} + \sum_j z_j n_j} \times 100 \quad (4.1)$$

$$\text{Selectivity to a product, } S_j(\%) = \frac{z_j n_j}{\sum_j z_j n_j} \times 100 \quad (4.2)$$

where z_j and n_j are the number of atoms of carbon and moles of gaseous carbon containing product j. $n_{propane}$ is the mole of unconverted propane in the product stream.

CHAPTER 5

RESULTS AND DISCUSSION

5.1 Catalyst Characterization

5.1.1 X-ray diffraction (XRD)

Fig. 5.1 shows the XRD patterns of the three VO_x/CaO-γAl_2O_3 catalyst samples (different CaO/γAl_2O_3 ratios) and bare CaO, γAl_2O_3 supports and V_2O_5 for comparison. The XRD pattern of V_2O_5 shows well-defined crystal structures at 2θ angles of 12.8°, 17.4°, 19.7°, 24.1°, 28.2°, 43.3° and 48.2°. The γAl_2O_3 samples gives two peaks at 2θ angles of 48° and 67°, which is consistent to the previous studies [27]. The XRD pattern of CaO shows well-defined reflections at 2θ angles of 32°, 38° and 55°, this is also in line with the literature [63]. The XRD pattern of the three catalysts samples show no peaks corresponding to the vanadium oxide species. The similar XRD patterns of VO_x/CaO-γAl_2O_3(1:4) and VO_x/CaO-γAl_2O_3(1:1) samples further confirmed the non-crystalline appearance of VO_x species. This can be ascribed to the fact that the VO_x species in the catalyst samples has highly dispersed amorphous phase on the γAl_2O_3 and CaO surface. There is also another possibility of presence of small XRD undetectable V_2O_5 crystalline nanoparticles with high level of dispersion on the γAl_2O_3 and/or CaO support. This observation is consistent to the finding available in the literature [18]. The other probable phases, AlV_2O_9 and CaV_2O_6 phases were also not detected in any of the catalyst samples. One can infer from this

observation that the reaction between vanadium and the support materials γAl_2O_3 and/or CaO is negligible during the treatment even at 750 ^oC.

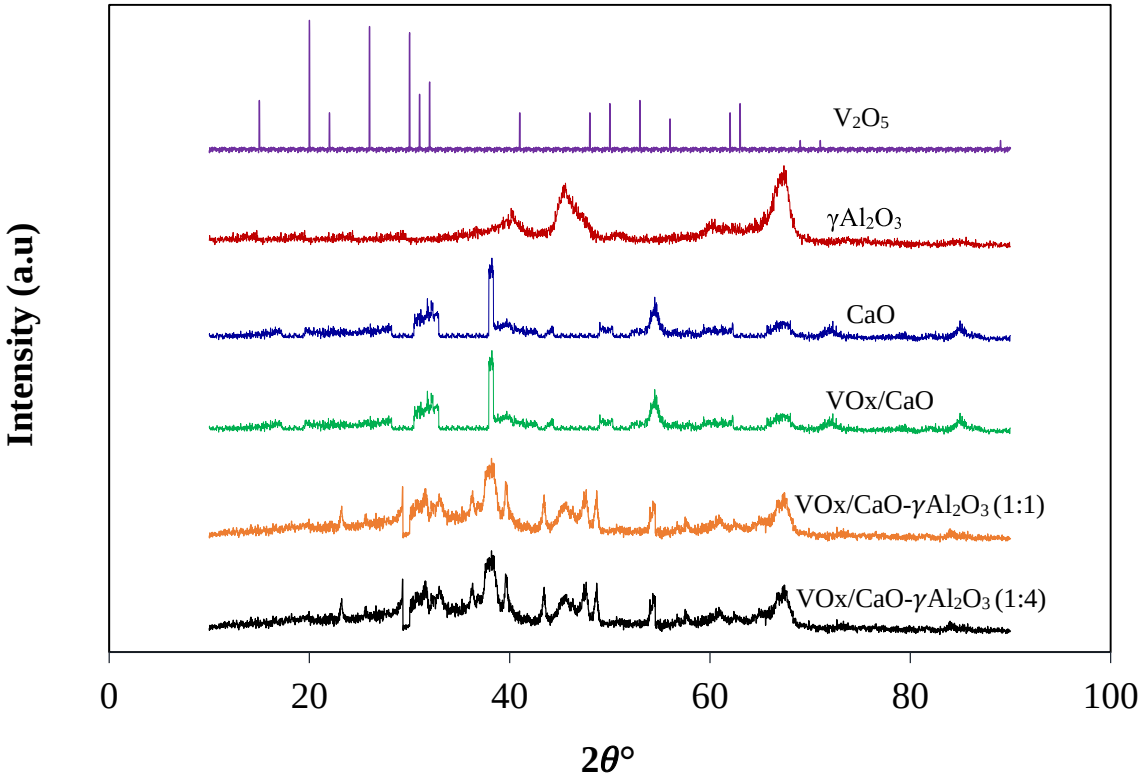

Fig. 5.1: XRD patterns of all three catalyst samples and their components

5.1.2 Laser Raman Spectroscopy

The Raman spectra of the samples were obtained at ambient temperature presented in Fig. 5.2. This figure also includes the Raman spectra of bare CaO and γAl_2O_3 supports and V_2O_5 samples. The Raman spectra analysis suggests that all the three catalyst samples contains both monovanadate and polyvanadate with minute crystal particles of V_2O_5. The broad bands in the range of 670-945 cm^{-1} is attributed to stretching mode of V-O-V. The 945-1030 cm^{-1} band is ascribed to the stretching mode of V=O [27]. The narrow 1030-1035 cm^{-1} band is ascribed to stretching mode of the V=O bond in isolated monovanadate surface species. All other bands appearing around 100, 235, 325, 345, 448, 520, 567, 993 cm^{-1} are ascribed to bulk V_2O_5 crystals. In addition, all the catalyst samples have slight peaks at 1030-1035 cm^{-1} which is monovanadate species [27].

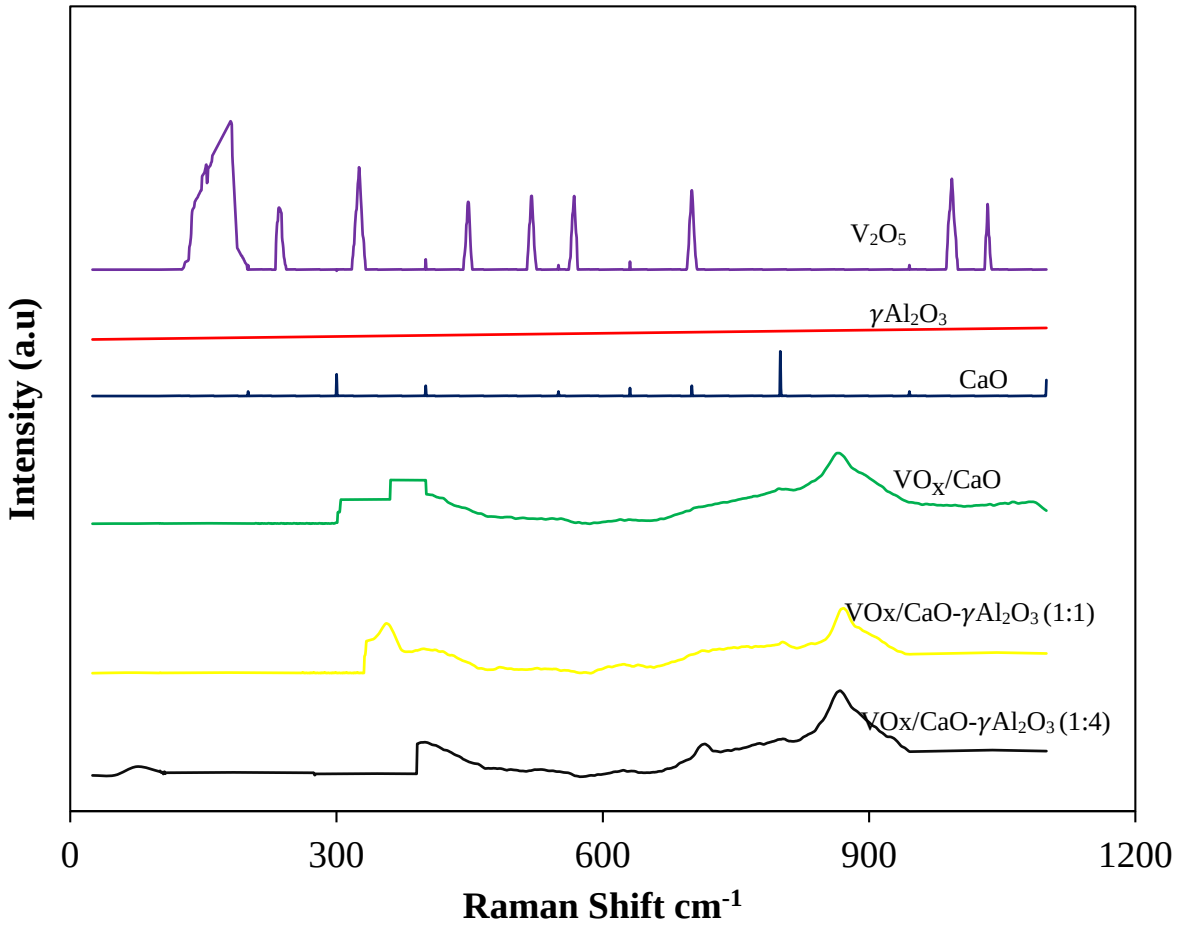

Fig. 5.2: Raman spectra of the three catalyst samples and their components

5.1.3 FTIR Analysis

Fig. 5.3 displays the FTIR spectra of VOx/CaO-γAl_2O_3 (1:4), VOx/CaO-γAl_2O_3 (1:1) and VOx/CaO catalysts and CaO, γAl_2O_3, V_2O_5 samples for comparison. The strong infrared bands at 3464, 1629, 821 as shown in the FTIR spectra representing γAl_2O_3. These peaks are attributed to stretching vibration of Al-O bond [64]. There are also strong infrared band

at 450 cm^{-1} as shown in CaO curve. This peaks may be attributed to the lattice vibrations of CaO [64, 65]. Strong infrared absorption bands were observed at 833, 1014 and 1629 cm^{-1} on the V_2O_5 curve. The peak at 1014 cm^{-1} corresponds to strong terminal oxygen bond (V^{5+}=O) [66]. The absorption peak at 450 cm^{-1} in all three catalyst samples, VOx/CaO-γAl_2O_3 (1:4), VOx/CaO-γAl_2O_3 (1:1) and VOx/CaO confirms the presence of CaO in the catalysts. The band at 1629 cm^{-1} confirms the presence of V_2O_5 in the catalyst samples and the band at 821 cm^{-1} confirms the presence of γ Al_2O_3 in the catalyst samples.

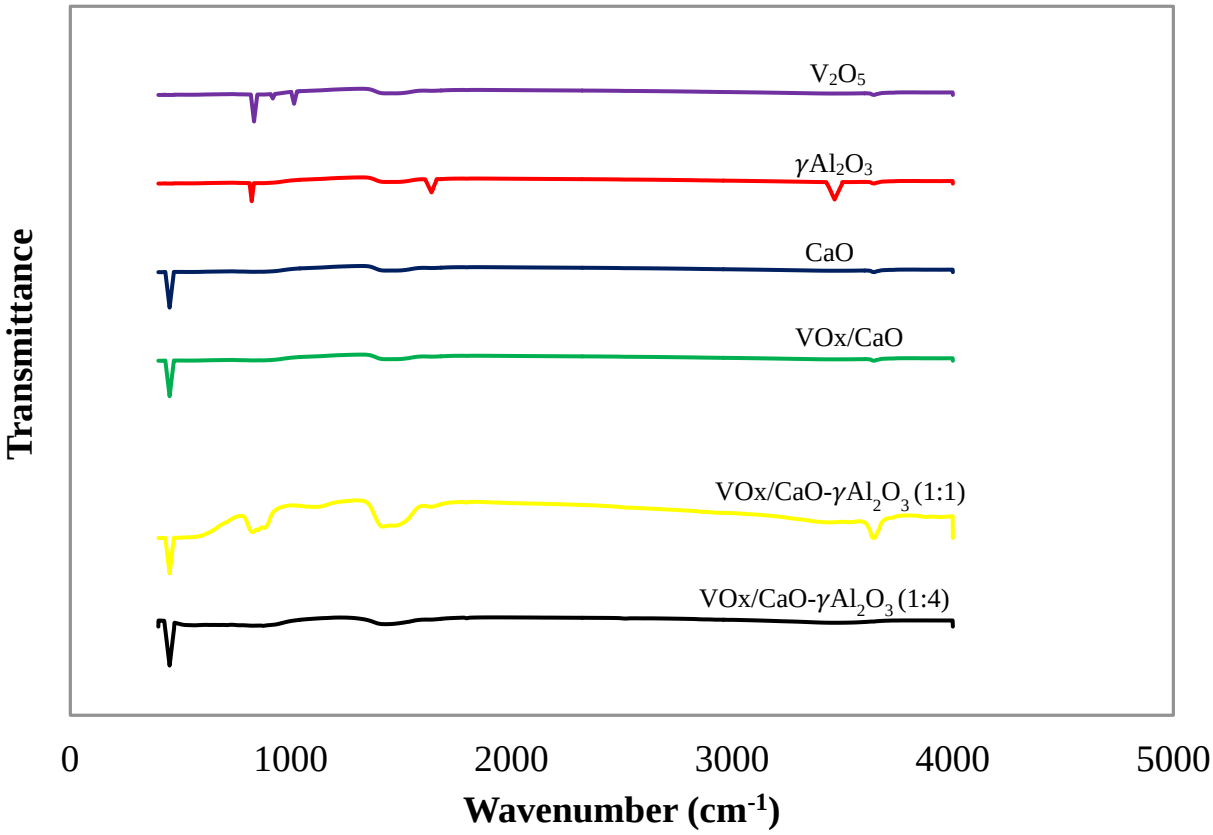

Fig. 5.3: FTIR absorption spectra of the three catalyst samples and their components

5.1.4 Reduction and Oxygen Carrying Capacity

TPR/TPO is an important technique for the characterization of gas phase oxygen free ODH catalysts given it simulates, reduction/oxidation of the catalysts as expected during the actual ODH reaction with ethane (Eq. 5.1 and Eq. 5.2).

TPR:

$$V_2O_5 + 2\ H_2 \rightarrow V_2O_3 + 2\ H_2O \quad (5.1)$$

ODH of propane:

$$2C_3H_8 + V_2O_5 \rightarrow 2C_3H_6 + 2H_2O + V_2O_3 \quad (5.2)$$

One can see that both the TPR (Eq. 5.1) and ODH of propane (Eq. 5.2) reduce V_2O_5 to V_2O_3. On the other hand, the TPO cycle (Eq. 5.3) represents the catalyst regeneration cycle following the reduction in TPR.

TPO:

$$V_2O_3 + O_2 \rightarrow V_2O_5 \quad (5.3)$$

In addition, the TPR/TPO data can be further processed to determine the oxygen carrying capacity of the catalysts for the oxidative dehydrogenation of propane without any additional gas phase oxygen (catalyst reduction cycle). Therefore, TPR analysis indicates the temperature range of catalyst activation and amount of available lattice oxygen for ODH of propane.

Fig. 5.4 presents the TPR profiles of the $VO_x/CaO\text{-}\gamma Al_2O_3$ catalyst with different CaO to γAl_2O_3 ratios. One can see that all the three catalyst samples have similar reduction profiles

and reduces between 350 to 620 °C. The single peak attributed to each catalyst samples shows the presence of amorphous monomeric and polymeric species of VO_x surface and the absence of crystalline V_2O_5 nanoparticles, which gives indication of high reducibility. For all the catalyst samples, there was no peak attributed to CaO or Al_2O_3. This is due to the fact that calcium and aluminum are higher in the electrochemical series as compared vanadium and hydrogen. The temperature that will be required for reduction of CaO and Al_2O_3 with hydrogen is higher than the temperature range considered in the TPR experiment. However, the reduction peak temperatures of the samples significantly varied with the variation of the CaO content in the catalyst formulation. The peak temperature of the lowest CaO containing VO_x/CaO-γAl_2O_3 (1:4) sample was 515 °C. With increasing the CaO content, VO_x/CaO-γAl_2O_3 (1:1) sample, the peak temperature shifted to 560 °C. The CaO supported VO_x/CaO sample shows highest peak temperature at 583 °C. Previously, Bosc et al. [50] and Koranne et al. [51] reported similar reduction behavior of CaO containing vanadium catalysts.

TPR data was further processed to evaluate the degree of reduction for the three catalyst samples. The degree of reduction can be defined as the percentage of VO_x reduced to the actual quantity of vanadium oxide available in the catalyst. The exposed reducible VO_x was calculated from the amount of hydrogen uptake evaluated using numerical integration of the resulting temperature programmed reduction peak area. The mass of reducible vanadium oxide in the catalyst sample was evaluated using molar volume of gas at STP, volume of hydrogen uptake, molecular weight of vanadium oxide and stoichiometric

number of hydrogen in the gas-solid reaction involved in reduction. The percentage of vanadium oxide reduction can be calculated using the following relation:

$$\%\ \text{reduced} = \frac{Mw_v \times V_{H_2}}{v \times V_g \times W_o} \times 100 \qquad (5.6)$$

where (1)W_V is the amount of reduced vanadium (g), (2) Mw_v is the molecular weight of vanadium (g/mol), (3) V_{H_2} is the volume of reacted hydrogen (cm^3 at STP), (4)V_g is the molar volume of gas(mol/cm^3 at STP). (5) W_o is initial weigh of vanadium (g) and (6) v is the stoichiometric number of hydrogen based on the following reaction stoichiometry. Assuming that V_2O_5 is the initial reducible catalyst species present on the support, then the following reduction equation applies:

$$V_2O_5 + 2H_2 \rightarrow V_2O_3 + 2H_2O \qquad (5.7)$$

Table 5.1 shows the hydrogen uptake and the percentage reduction of the catalyst samples. One can see form this table that the hydrogen uptake was increased with the increasing the CaO content in the catalyst samples. This is due to the fact that the catalyst with higher quantity of CaO has higher basicity. The hydrogen gas in solution is acidic and will have higher reactivity with catalyst of high basicity.

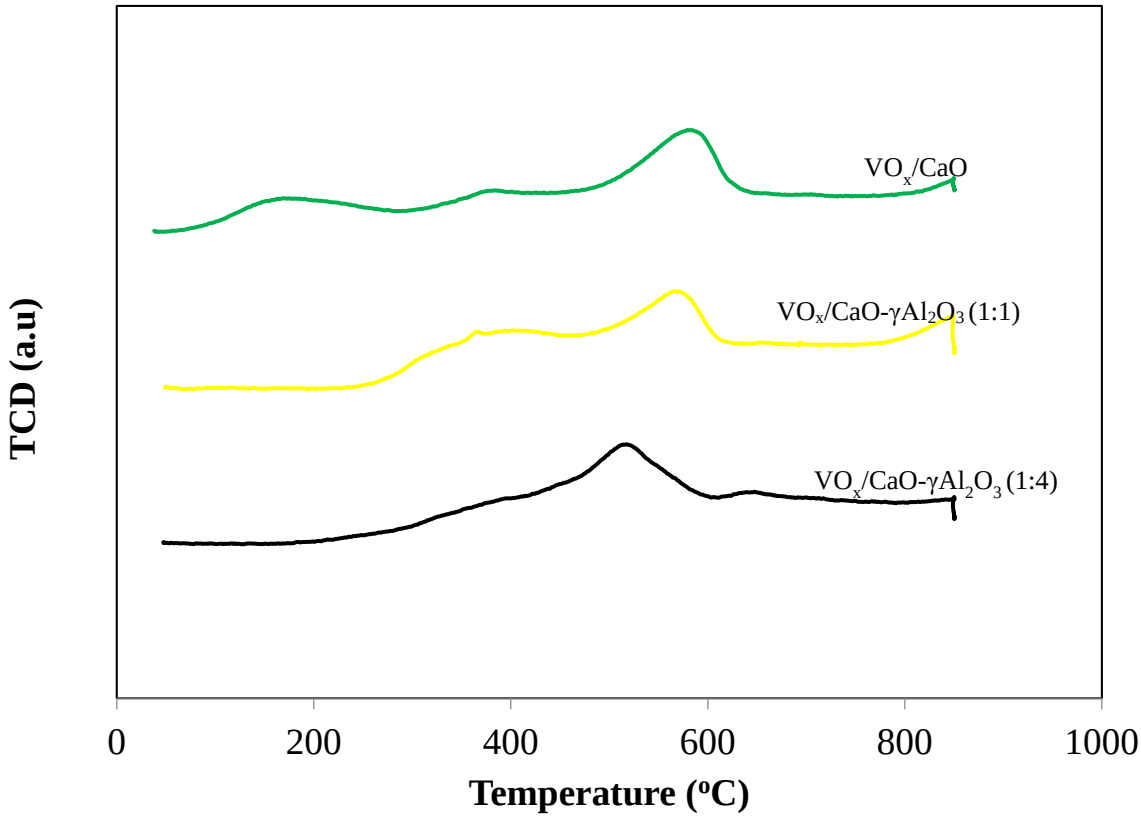

Fig. 5.4. Temperature programmed reduction profiles of $VO_x/CaO-\gamma Al_2O_3$ catalyst samples

Table 5.1: TPR Data comparing hydrogen consumption for all the catalyst samples

Sample	Uptake of H_2 (cm^3 STP)	% reduction
VO_x/CaO-γAl_2O_3 (1:4)	2.12	48.21
VO_x/CaO-γAl_2O_3 (1:1)	2.87	65.27
VO_x/CaO	3.18	72.32

In order to observe the stability under redox cycles, the catalysts samples were exposed in consecutive reduction and re-oxidation cycles. For all three catalyst samples, the hydrogen uptake remain consistent over the repeated TPR/TPO cycles although the percentage reduction of each sample varied as discussed above. The stable value of the hydrogen consumption suggests the stability of the present catalysts.

5.1.5 NH_3-TPD

The acid sites of the three catalyst samples were characterized by TPD using NH_3 as the basic probe molecule. The area of the TPD curve peak gives acid amount while the position of the peak indicates the acid distribution in the catalyst samples. Ammonia TPD can distinguish sites only by sorption strength, hence its shortcoming lies in its inability to differentiate between Lewis and Bronsted acid sites. Ammonia was used in this research work to make comparison of the total acidity and acid strength for the catalyst samples with different CaO/Al_2O_3 ratio. Fig. 5.5 shows the relationship between the desorption

volume as function of the temperature. One can easily see that all three samples show similar TPD profiles although the peak intensity and desorption peaks were shifted with the variation of CaO/Al_2O_3 ratios. The NH_3-TPD profile for $VOx/CaO\text{-}\gamma Al_2O_3$ (1:4), $VOx/CaO\text{-}\gamma Al_2O_3$ (1:1) and VOx/CaO samples showed an initial desorption peak at 183, 300, 302 ^oC followed by a high temperature desorption peak at 676, 636 and 620 ^oC, respectively. Clearly, the intensity of the high temperature desorption peaks were significantly higher than that of the low temperature peak. This indicates that percentage of the strong acid sites are much higher than the weak acid sites. The total acidity of each samples were calculated by integrating the calibrated TPD profiles. Table 5.2 shows the uptake of NH_3 by the three catalyst samples and their respective temperature of desorption. Expectedly, the total acidity of the samples were decreased with the increase of the CaO content due to the basic nature of the CaO.

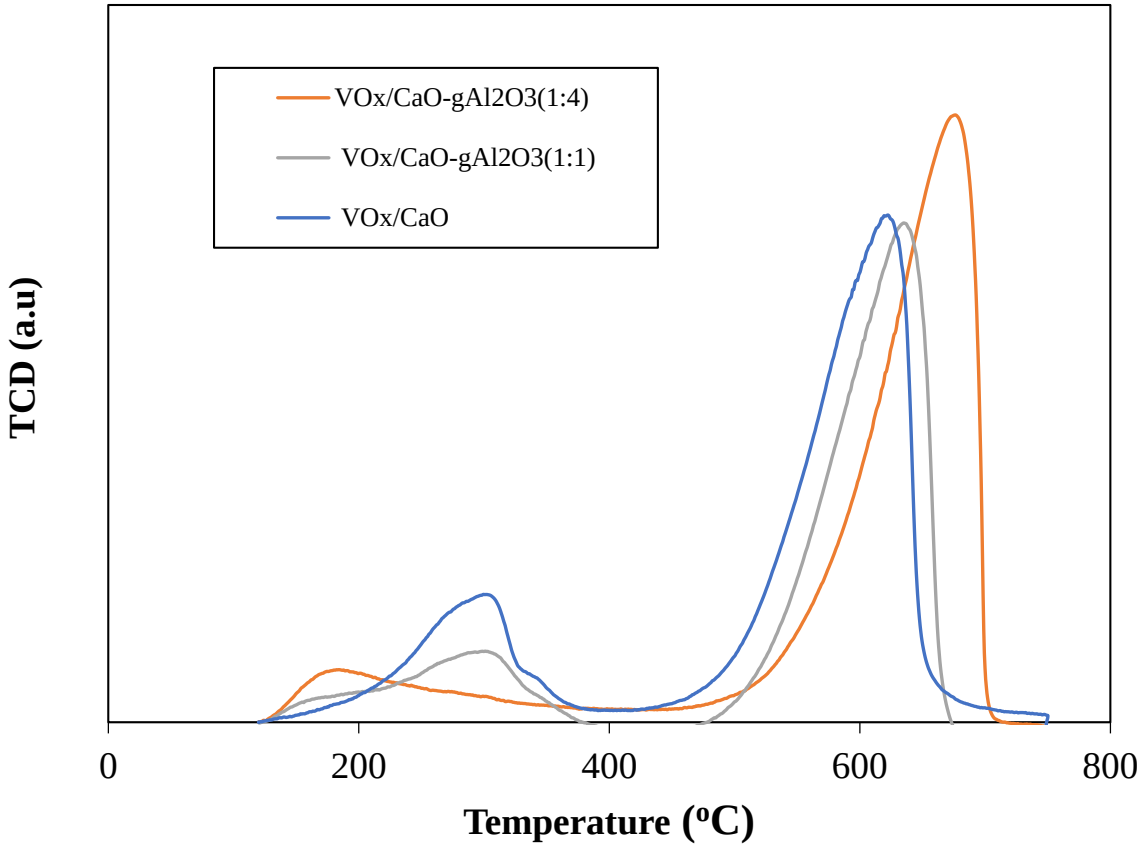

Fig. 5.5: NH_3-Temperature programmed desorption profiles for the catalyst samples

Table 5.2**:** Catalyst acidity as measured by NH_3-TPD

Catalyst Sample	Peak temperatures ^oC		NH_3 Uptake (mmol/g)		
	Low Temp	High Temp	Low Temp	High Temp	Total
VOx/CaO-γAl_2O_3(1:4)	183	676	0.0133(17%)	0.0666(83%)	0.0799
VOx/CaO-γAl_2O_3(1:1)	300	636	0.0163(21%)	0.0612(79%)	0.0775
VOx/CaO	302	620	0.0190(26%)	0.0539(74%)	0.0729

5.1.6 NH_3-TPD Kinetics

Ammonia desorption kinetics was conducted to determine metal-support interaction of the catalyst samples. The activation energy of ammonia desorption and the pre-exponential factors were estimated by modeling the NH_3-TPD experimental data of each catalyst sample. Cvetanovic and Amenomiya described desorption rate as a function of temperature which is based upon the following assumptions:

(i) Temperature (T) of desorption has linear relationship with time (t).

(ii) The rate of desorption is of first order in coverage.

(iii) The concentration of ammonia gas through the catalyst bed is uniform

(iv) Desorbed ammonia has zero feasibility for re-adsorption

(v) The catalyst's surface is homogenous for the NH_3 adsorption, which means desorption constant, $k_d = k_{do} \exp(-E/RT)$. The desorption constant is independent of the surface coverage.

Suitable experimental conditions were selected in order to satisfy the assumptions in (i) and (iii). High flow of Ammonia gas through the catalyst bed was maintained in order to satisfy the assumption in (iv). Unimolecular desorption of ammonia were assumed in order to consider the assumption in (ii).

Ammonia desorption rate at a uniform first order energy of desorption can be evaluated using a component balance of desorbing NH_3.

$$r_d = -V_m \frac{d\theta}{dt} = k_{do}\theta \, exp\left[-\frac{E}{R}\left(\frac{1}{T} - \frac{1}{T_m}\right)\right] \tag{5.8}$$

Where, T_m is the centering temperature in ^oC, V_m is the volume of NH_3 adsorbed at saturated conditions in ml/g, V_d is the volume of ammonia desorbed at different temperatures in ml/g, θ is the surface coverage of the adsorbed species, E is the energy of ammonia desorption in kJ/mol, K_d is desorption constant in ml/(g.min) and K_{do} is the pre-exponential factor in ml/(g.min).

Temperature (T) in a TPD experiment has linear relationship with time (t).

$$T = T_o + \alpha t \tag{5.9}$$

where, T is desorption temperature at time (t).

$$\frac{dT}{dt} = \alpha \tag{5.10}$$

$$\frac{d\theta}{dt} = \frac{d\theta}{dT}\frac{dT}{dt} = \alpha\frac{d\theta}{dT} \tag{5.11}$$

$$\frac{d\theta}{dT} = -\frac{k_{do}}{\alpha V_m}\theta \exp\left[-\frac{E}{R}\left(\frac{1}{T}-\frac{1}{T_m}\right)\right] \quad (5.12)$$

$$\theta = 1 - \frac{V_d}{V_m} \quad (5.13)$$

$$\frac{dV_d}{dT} = \frac{k_{do}}{\alpha}\left(1-\frac{V_d}{V_m}\right) \exp\left[-\frac{E}{R}\left(\frac{1}{T}-\frac{1}{T_m}\right)\right] \quad (5.14)$$

The first order ordinary differential equation was solved using the variable separable method to obtain the resulting equation given as:

$$V_d = V_m\left(1 - exp\left[\ln\left(1-\frac{V_o}{V_m}\right) - \frac{k_d R T^2}{E\alpha V_m}\left\{exp\frac{-E}{R}\left(\frac{1}{T}-\frac{1}{T_m}\right) - exp\frac{-E}{R}\left(\frac{1}{T_o}-\frac{1}{T_m}\right)\right\}\right]\right) \quad (5.15)$$

V_o and T_o are initial volume desorbed in ml/g and initial desorption temperature.

R= universal gas constant in KJ/mol/K, The heating rate, α was taken as 10 ^oC/min

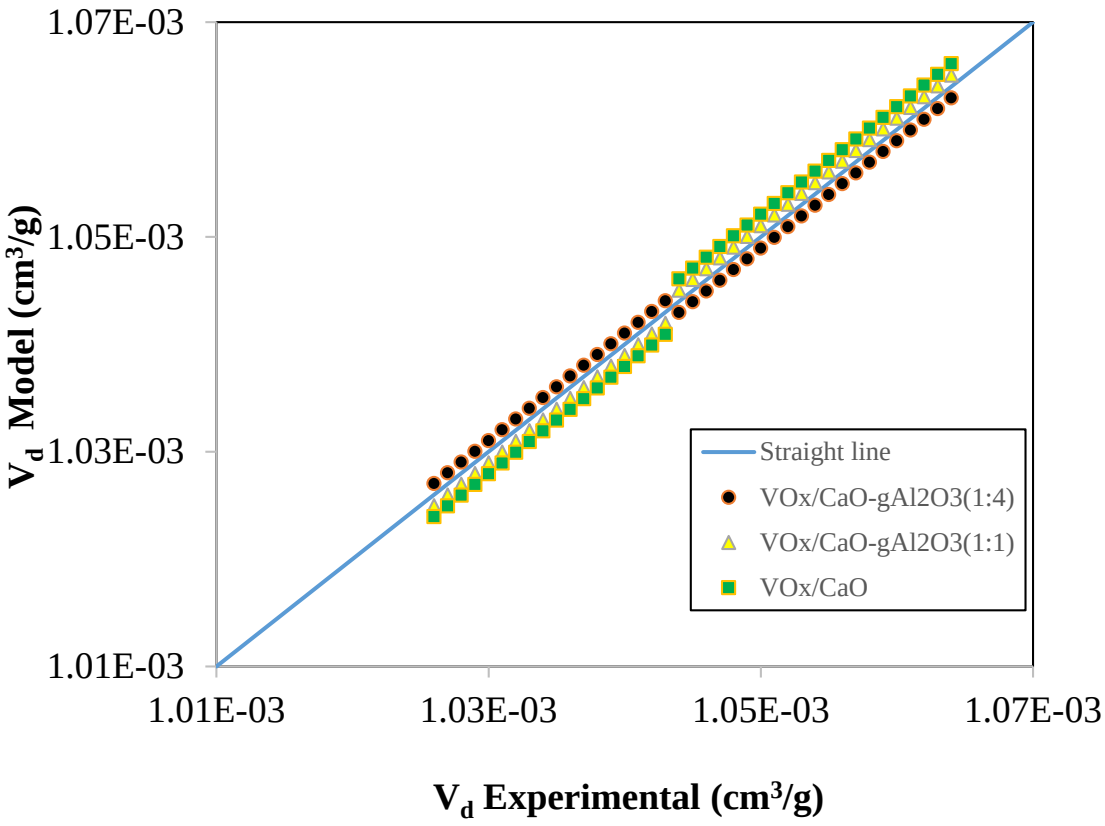

Fig. 5.6: Experimental Data and Fitted Model of ammonia desorption during NH_3-TPD for different catalyst samples

TPD data obtained from experiment and the proposed model have good agreement for all the catalyst samples as shown in Fig. 5.6. This proves the validity of the proposed desorption model. The TPD data was fitted in the resulting equation using the non-linear regression analysis on MATLAB. The desorption energies and pre-exponential factors of each catalyst sample were obtained. The norm of the residuals and the coefficient of

correlation were calculated for each catalyst sample using MATLAB and MINITAB software at 95 % confidence limit.

Table 5.3 Estimated parameters for ammonia-TPD kinetics at 10 ^{o}C/min

Sample	E(KJ/mol)	k_{do} (ml/g/min) $\times 10^5$	Norm of residuals $\times 10^4$	V_{NH3}(ml/g)
$VO_x/CaO\text{-}Al_2O_3$ (1:4)	39.2	3.8	2.1	72.6
$VO_x/CaO\text{-}Al_2O_3$ (1:1)	74.8	1.3	6.4	57.7
VO_x/CaO	96.3	0.5	22.7	47.6

The energy of desorption for the three synthesized catalyst were reported in Table 5.3. Statistical properties such as correlation coefficient R^2, Norm of residuals and 95% confidence intervals were considered in the analysis. The values of R^2 and residual norms for all the three catalyst are close to 1 and 0 respectively, which shows that the proposed desorption model is applicable.

The values in the table show that as the loading of CaO is increased and that of γAl_2O_3 is decreased, the energy of desorption increases. This can be explained based on the amount of ammonia uptake for each of the catalyst. The catalyst with the highest desorbed ammonia has the lowest desorption energy while the one with the lowest desorbed ammonia has the highest desorption energy. Similar observation was described by S. Ghamdi et al. [25] on γAl_2O_3 supported VO_x catalysts where higher desorption energy

corresponds to lower amount of NH_3 adsorbed from the catalysts. The increase in the activation energy can also be linked to the heterogeneity of the catalyst samples. The interaction between the mixed support and the active site also play significant role in the value of energy required for ammonia desorption. Weak interaction will enable high dispersion of the active site which will in turn leads to availability of the lattice oxygen for the ODH reaction. Hence a weaker active site-support interaction will require lower energy of desorption which means the catalyst with 2g CaO has the weakest active site-support interaction.

5.1.7 SEM-EDXS analyses

The scanning electron microscope (SEM) was carried out together with energy dispersive X-ray analysis (EDX). A representative field emission scanning electron microscopic image of one of the catalyst samples VOx/CaO-γAl_2O_3 (1:1) was presented in Fig. 5.7a. It shows the morphology of the catalyst. The images of the element distribution can be used to envisage the quality of the dispersion. The distribution of vanadium element over the oxygen carrier samples was shown in Figure 5.7b. It is evident that the vanadium particles are well dispersed on the CaO-γAl_2O_3 support. This indicates superior dispersion of the VOx over the CaO-γAl_2O_3 support.

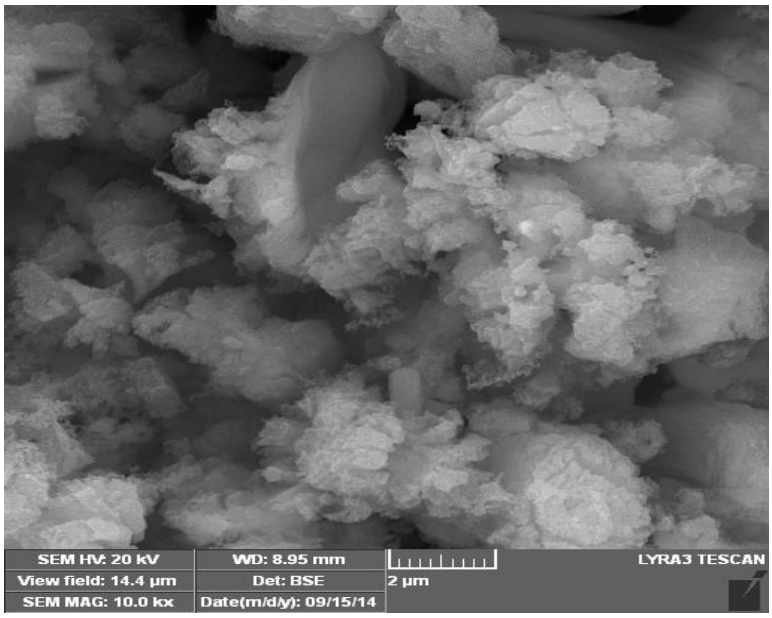

Figure 5.7a. SEM Images of VOx/CaO-γAl_2O_3

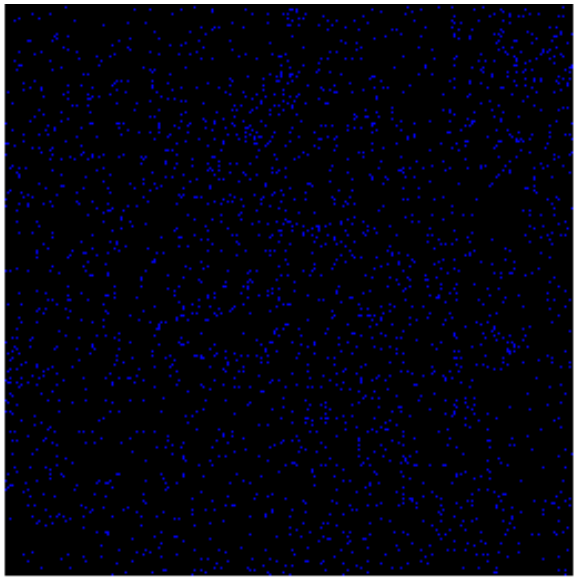

Figure 5.7b: Vanadium elemental mapping in VOx/CaO-γAl_2O_3(1:1) catalyst

5.2. Catalyst Evaluation

The gas phase oxygen free oxidative dehydrogenation (ODH) of propane experiments were conducted in a fluidized CREC Riser Simulator using pure propane (99.95% purity) as feed. Before performing the actual catalytic ODH runs, thermal experiments (without any catalyst) were conducted to confirm contribution of any thermal conversion. The highest reaction temperature (640 °C) was selected for the thermal experiments. The GC analysis of the thermal runs products showed mainly unconverted propane and a trace amount of ethane and methane most likely due thermal cracking of propane in absence of catalyst.

In the catalytic experiments, the reaction temperature was varied between 550 and 640 ^{o}C, while the reaction was attuned from 10 to 31 sec. The product analysis of the preliminary experimental runs contain unreacted propane, propylene and carbon dioxide. The propane conversion and product selectivity in the experimental repeats are found to be within 3.5% error limits. Mass balances were established for each experimental runs and the mass balances closed consistently in excess of 95%. From the product analysis, one can consider the following possible reactions steps during the fluidized ODH of propane runs in absence of gas phase oxygen:

ODH of propane to propylene: $2C_3H_8 + V_2O_5 \longleftrightarrow 2C_3H_6 + 2H_2O + V_2O_3$ (5.16)

Complete oxidation of propane: $C_3H_8 + 5V_2O_5 \longleftrightarrow 3CO_2 + 4H_2O + V_2O_3$ (5.17)

Complete oxidation of propylene: $C_3H_6 + \frac{7}{2}V_2O_5 \longleftrightarrow 2CO_2 + 3H_2O + V_2O_3$ (5.18)

Therefore, it is very important to identify the best reaction conditions in order to achieve highest possible propylene yields and suppress the complete combustion reactions which produce CO_2. Keeping the above in mind the following experiments were conducted at different conditions to demonstrate the effects of (i) the consecutive propane injection without catalyst regeneration (ii) reaction temperatures and (iii) contact times on the propane conversion and product selectivity.

5.2.1. Successive propane injections

The successive oxidative dehydrogenation of propane without catalyst regeneration experiments were conducted to demonstrate the effects of degree of catalyst reduction on the propane conversion and product distribution. To ensure the same reaction conditions,

the reactor was loaded with 0.5 g of catalyst and temperature was maintained at 640 °C. Further, in each run same 1.2 ml propane was injected and allowed the reactions to proceed for 17 sec. Fig. 8 plots the propane conversion and propylene and carbon oxides selectivity over the successive injection of propane runs. One can see from Fig. 5.8(a) that all three $VO_x/CaO\text{-}Al_2O_3$ catalysts give highest propane conversion in the first injection, which gradually decreased in the following successive propane injections. The availability of the oxygen in the catalyst surface mainly contributed to the high propane conversion in the first injection. The appreciable levels of catalyst activity after all the four successive injections can be attributed to the lattice oxygen availability in the catalyst matrix. On the other hand, the diminishing trends of the propane conversion is due to the progressive consumption of the lattice oxygen in the catalysts. Among the three catalysts, $VO_x/CaO\text{-}\gamma Al_2O_3$ (1:1) displays highest propane conversion (51 %), which is consistent to its highest oxygen carrying capacity compared to the other two catalysts as observed in TPR analysis.

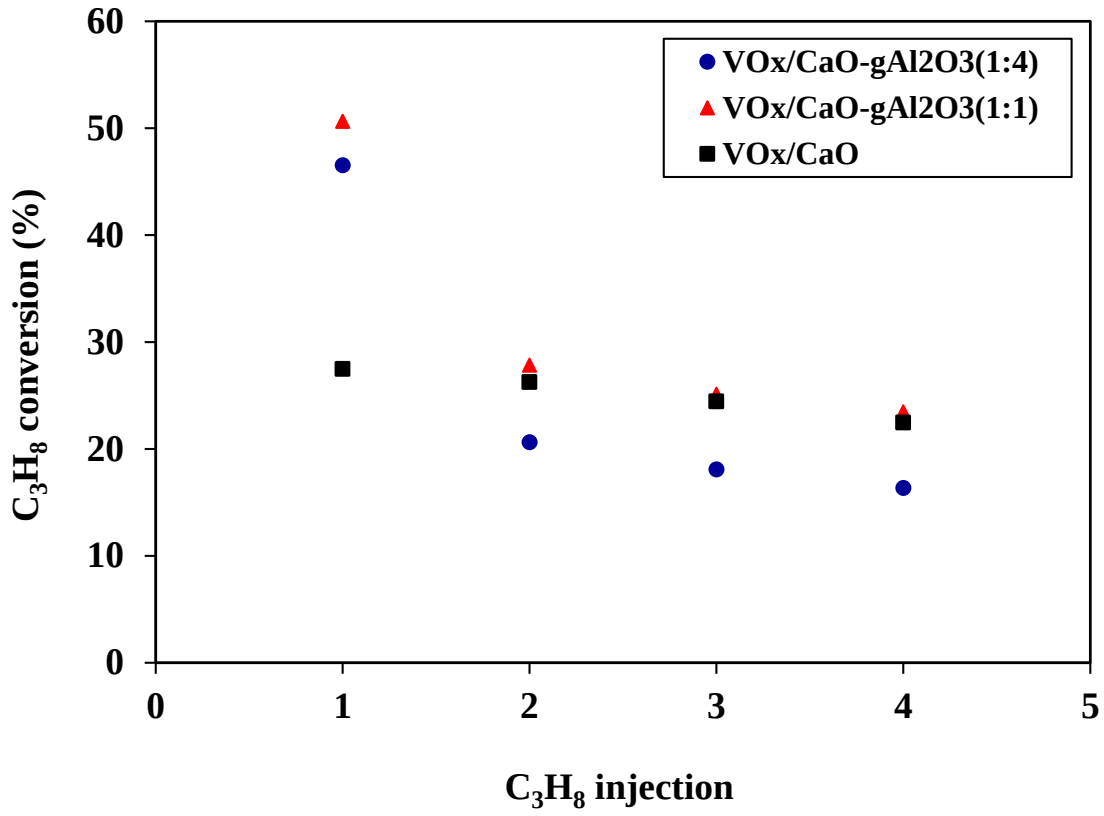

Fig. 5.8a. Conversion of propane in successive propane injection without catalyst regeneration (T: 640 °C; Catalyst: 0.5 g; Propane injected: 1.2 ml, Time: 17s)

The selectivity of both the desired propylene and undesired carbon dioxide also significantly varies during the successive propane injection runs as seen in Fig. 5.8(b). Unlike propane conversion, the first injection gives lowest propylene selectivity and highest carbon dioxide selectivity. This indicates that the surface oxygen favors the complete oxidation of propane/propylene producing carbon dioxide. The propylene selectivity significantly increased in second injection after that the increment become minimal in the remaining runs although there is an increasing trend still evident. This

variation in selectivity indicates that an optimum level of lattice oxygen is required to maximize selectivity to propylene and minimize selectivity to carbon dioxide.

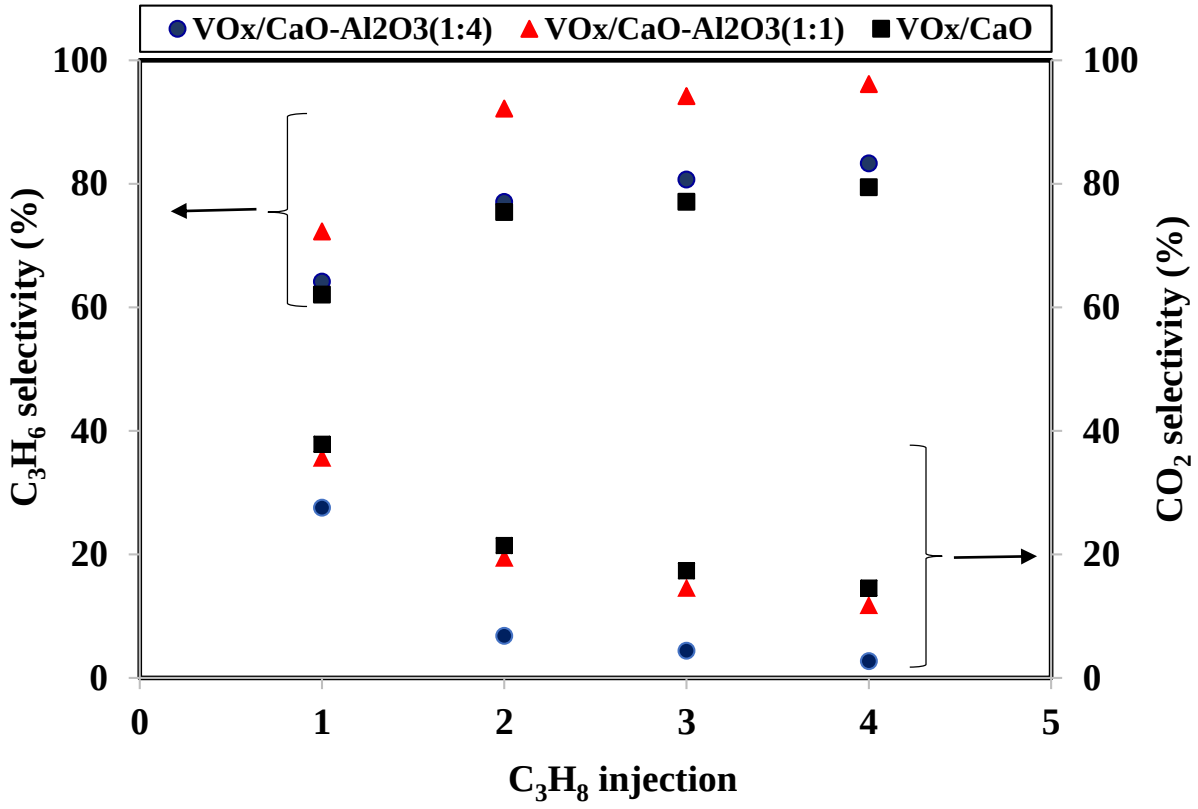

Fig. 5.8b. C_3H_6 and CO_2 selectivity in successive propane injection without catalyst regeneration (T: 640 °C; Cat.: 0.5 g; Propane injected: 1.2 ml, Time: 17s)

The above observation are in line with the fact that selectivity to propylene in oxidative dehydrogenation of propane over VOx based catalysts is intensely affected positively by the energy that binds the lattice oxygen with the catalyst [69]. At higher oxidation state of the catalyst the binding energy of the lattice oxygen is low, which eventually leads to

combustion of propane/propylene to carbon oxides. Furthermore, the surface oxygen on the fresh or regenerated catalyst are loosely bonded with the catalysts which easily reacts with propane/propylene to produce carbon dioxide. In this case, a selective catalyst surface would be obtained only after the adsorbed oxygen had been consumed via the first propane injection. It was after the consumption of adsorbed oxygen through the first propane injection that high selectivity catalyst surface would be obtained.

When compared, $VO_x/CaO\text{-}\gamma Al_2O_3$ (1:1) shows significantly higher propylene selectivity and much lower carbon dioxide selectivity. This catalysts shows up to 96 % propylene selectivity while the higher CaO containing catalysts produces up to 83 % propylene. This can be attributed to the moderate level of acidity of $VO_x/CaO\text{-}\gamma Al_2O_3$ (1:1) as depicted in the NH_3-TPD result. This observation is also consistent to the XRD and TPR results. The proper balance of CaO/Al_2O_3 influences the VO_x dispersion forming more isolated non-crystalline VO_x species, which favors the propylene formation and suppress the complete oxidation to CO_2. Furthermore, the increased V-support interaction with the CaO promoted sample, as revealed by the TPD kinetics analysis, also explain the control ODH reaction with the lattice oxygen of the catalyst, resulting enhanced propylene selectivity. Numerous works has been published on ODH selectivity as a function of oxidation state of vanadium based catalysts [6, 36, 66, 69-72]. This published works were focused on ODH reaction that utilizes successive injections of alkanes in the absence of gas phase oxygen and it proves that high selectivity for alkenes in ODH reaction can be obtained at optimum lattice oxygen of the vanadium based catalyst. Lopex-Nitro et al. [36] founds that the selectivity to propylene and butylene with respective usage of propane and butane as the

feed could be strongly influenced by the reducibility of the vanadium based catalyst. Balcaen et al. [73] also observed the same trend for ODH of propane over vanadium based catalyst. Ethane ODH over γ-Alumina supported vanadium catalyst in the absence of oxygen by Al-Ghamdi et al. [6, 69] also confirm that the absence of gas-phase oxygen is important for the selective conversion of alkane to alkene with the binding energy of lattice oxygen as the main driver of the reaction.

5.2.2. Effect of reaction temperature

Fig. 5.9 presents propane conversion and products (desired propylene and undesired carbon dioxide) selectivity at different reaction temperature and constant 17 sec reaction time. Expectedly, propane conversion increased with the increasing reaction temperature as the lattice oxygen of the catalyst activates at higher temperature (Fig. 5.4, TPR analysis). Interestingly, with increasing the reaction temperature, all the catalyst showed increased propylene selectivity and decreased carbon dioxide selectivity (Fig. 5.8(b)). The variation in the degree of reduction of the catalyst with reaction temperatures was responsible for the rise in the selectivity of propylene. At higher temperatures, the degree of catalyst reduction increases (Fig. 5.4, TPR analysis) a result of the lower binding energy of lattice oxygen. At such higher degrees of reduction of the catalysts, the selective pathway toward ODH is preferred over that for combustion as observer in the successive propane injection experiments. The good selectivity to propylene can also be attributed to the non-formation of larger molecules due to the interaction of the mixed support and the active site of each catalyst, as detected by XRD. Among the three studied catalysts, VOx/CaO-γAl_2O_3 (1:1)

shows highest propylene selectivity. The carbon dioxide selectivity with this catalysis is also lower than that of the VOx/CaO catalyst while slightly higher than the VOx/CaO-γAl_2O_3 (1:4) catalyst. The superior propylene selectivity of the VOx/CaO-γAl_2O_3 (1:1) is can be attributed to the moderate level of acidity of VOx/CaO-γAl_2O_3 (1:1) as depicted in the NH_3-TPD results.

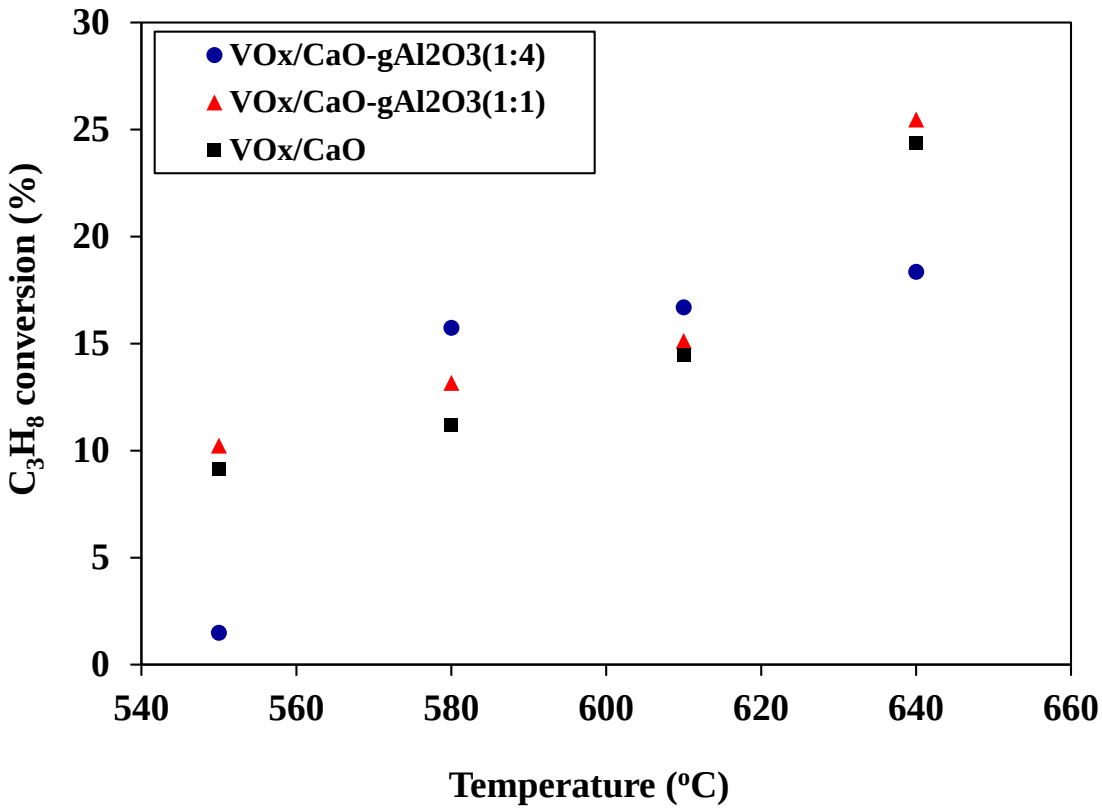

Fig. 5.9a. Conversion of propane at different temperature (Cat.: 0.5 g; Propane injected: 1.2 ml, Time: 17s)

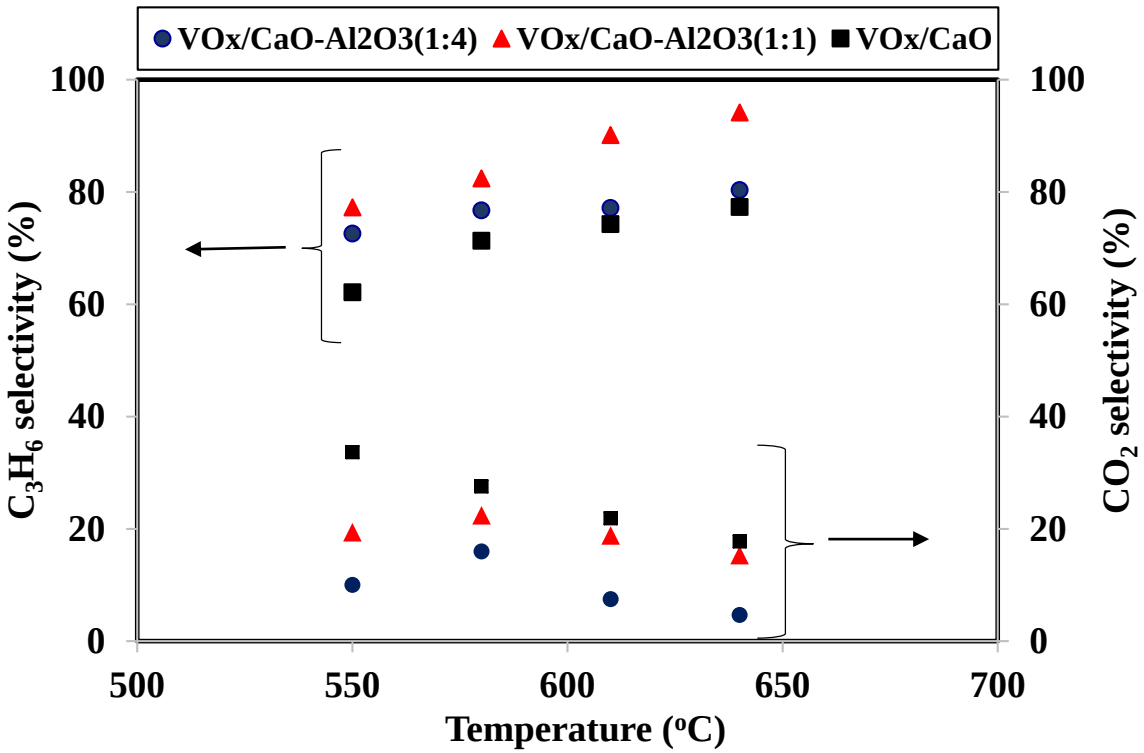

Fig. 5.9b. C_3H_6 and CO_2 selectivity at different temperature (Cat.: 0.5 g; Propane injected: 1.2 ml, Time: 17s)

5.2.3. Effect of reaction time

Propane ODH experiments were carried out at 10, 17, 24 and 31 s in order to study the effect of reaction time on propane conversion, propylene selectivity and carbon oxides selectivity at the best temperature, 640 °C. It is perceived that propane conversion for all catalysts rises with the reaction time as shown in Fig. 5.9(a). The propylene selectivity slightly increases from 10 to 17 sec and after that it decreases with reaction time. Conversely, the carbon dioxide selectivity oxide slightly decreases from 10 to 17 sec and increases from 17 to 31 sec (Fig. 5.9(b)).

Therefore, the higher contact times favor high propane conversions while optimum or moderate contact time favors high propylene selectivity and low carbon oxide selectivity. The good selectivity to propylene obtained from the three catalyst can be attributed to the high proportion of monovanadate VOx species which was detected from the Laser Raman Spectroscopy result. Again, VOx/CaO-γAl_2O_3 (1:1) shows the highest propane conversion and propylene selectivity and lowest carbon oxide selectivity. This can be attributed to the moderate level of acidity of VOx/CaO-γAl_2O_3 (1:1) as depicted in the NH_3-TPD result.

Thus, one can conclude that the performance of the VO_x/CaO-γAl_2O_3 (1:4), VO_x/CaO-γAl_2O_3 (1:1) and VO_x/CaO catalyst samples is strongly influenced by both reaction times and temperatures and also catalyst regeneration. It can be inferred that successive feed injections are the best for ODH reaction, hence it is only on completion of the successive reaction cycles that catalyst should be regenerated. This can be applied industrially using a fluidized bed reactor that has reactor-regenerator compartments where only small percentage of the catalyst have the ability of being transferred to the regenerator.

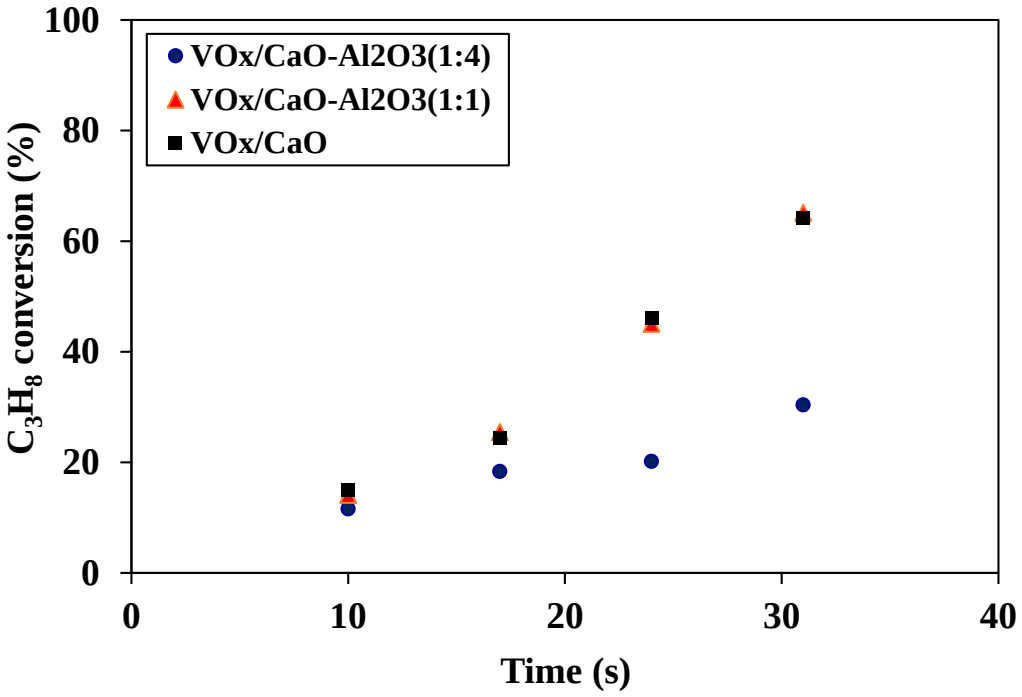

Fig. 5.10a. Conversion of propane at different reaction time (Cat.: 0.5 g; Propane injected: 1.2 ml, T: 640 ^{o}C)

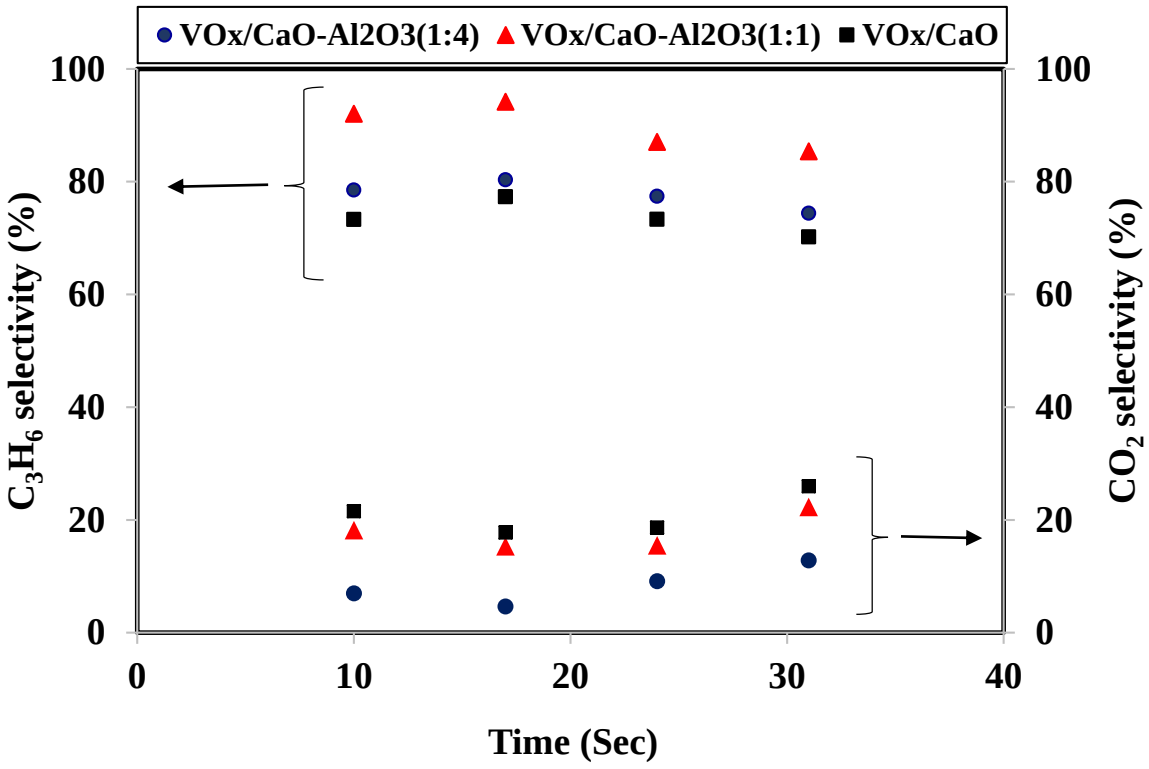

Fig. 5.10b. C_3H_6 and CO_2 selectivity at different reaction time (Cat.: 0.5 g; Propane injected: 1.2 ml, T: 640 ^oC)

CHAPTER 6

KINETIC MODELLING

6.1 Introduction

The chapter presents the use of VOx/CaO-γAl_2O_3 catalysts in establishing ODH kinetics of propane using surface lattice oxygen in a CREC Riser Simulator. It started with a proposed mechanism of propane ODH reaction by highlighting and confirming the main assumptions of the proposed kinetic model. The resulting system of partial differential equations is derived based on the proposed kinetic model assumptions. The results obtained from the kinetic models which include a number of parameters were analyzed in detail.

6.2 Data Analysis

The result obtain from the propane ODH reaction runs as shown in Fig 5.9 a and 5.9 b depicts the variation of conversion of propane, selectivity of the desired propylene and selectivity of undesired carbon (IV) oxide with temperature that ranges from 550 ^oC to 640 ^oC for all the catalyst samples. The conversion of propane increases with temperature due to the increased activation of lattice oxygen at high temperature. The selectivity of desired propylene increases with temperature, which is in line with the increased degree of reduction and desorption with temperature as depicted from TPR and TPD figures. The increase in the propylene selectivity can also be attributed to the non-formation of larger

molecules due to the interaction of the mixed support and the active site as detected by XRD.

The result obtain from the propane ODH reaction runs as shown in Fig 5.10a and 5.10 b depicts the variation of conversion of propane, selectivity of the desired propylene and selectivity of undesired carbon (IV) oxide with reaction time that ranges from 10 s to 34 s for all the catalyst samples at the best temperature (640 ^{o}C)

The conversion of propane increases from 10 s to 34 s, while the selectivity of propylene increases slightly from 10 to 17 s and decreases from the 17 s to 31 s for all the three catalyst samples. The increase in propane with time is expected because higher times will lead to higher period of exposure of propane with surface lattice oxygen. The selectivity decrease from 17s to 31 s shows optimum reaction time is required for higher selectivity of propylene and lower selectivity.

The decrease in the selectivity of propylene with time with a corresponding increase in the selectivity of carbon (IV) oxide shows that the primary product of the ODH reaction is propylene, while the secondary product of the combustion of propane and propylene is carbon (IV) oxide. ODH of propane entails of series and parallel reaction networks, which are (a) the desired oxidative dehydrogenation of propane to propylene and water, (b) the undesired primary combustion of propane to carbon oxides and water and (c) the undesired secondary combustion of propylene to carbon oxides and water. The desired ODH of propane and the undesired secondary combustion of propylene are in series while the desired propane ODH and the undesired primary combustion of propane are in parallel. A reaction network is proposed with the ODH of propane, primary combustion of propane

and secondary combustion of propylene product having rate constants k_1, k_2 and k_3 respectively as shown below.

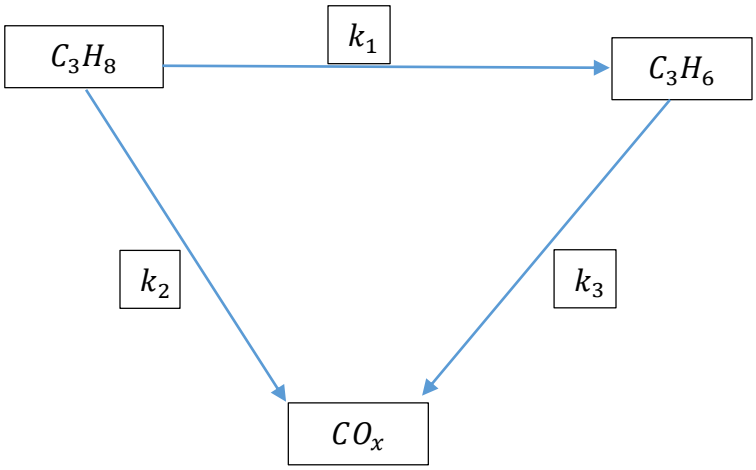

Fig 6.1. Proposed network of series and parallel reactions in the ODH of propane over Vanadium Oxide supported on CaO and CaO/$\gamma - Al_2O_3$ in a riser simulator

6.3. Model development

In order to develop an effective kinetic model in this present study, it was hypothesized that it is only the surface lattice oxygen on the catalyst that take part in the series and parallel network of reactions involved in the ODH of propane. On the basis of this postulate, the surface lattice oxygen was incorporated in the kinetic model. Moreover, an allowance must be made for the catalyst's time on stream or catalyst history in order to achieve a kinetic model capable of describing all transient observations during the course of the ODH reaction. An expression that is based on the fraction of the original oxygen remaining after the propane ODH reaction was used to give allowance for the catalyst's

time on stream. This is of utmost importance in order to accomplish a kinetic model that can describe all momentary observations in that occurred in the reaction. The expression can be termed as time dependent degree of oxidation of ODH catalyst and it is expected to decrease for consecutive reactions provided there is no catalyst regeneration.

De lasa and Al-Khattaf, Hossain et al proposed a kinetic model that utilizes an exponential decay function that incorporate the catalyst's degree of oxidation. A similar approach is proposed in this present study. The catalyst degree of oxidation is represented as a function of the conversion of propane. Here, the propane conversion has lots of benefit due to dependence of reaction time and temperature. The relation is given below

$$\tau = e^{-\lambda(X_{C_3H_8})} \tag{6.1}$$

Where the percentage conversion of propane is denoted by $X_{C_3H_8}$, λ is the decay constant and τ is the catalyst's degree of oxidation.

The choice of kinetic model for oxidative dehydrogenation of propane is of utmost significance. Owing to this fact, a mechanism that is suitable for reactions that some of its products leave the surface of the catalyst with one of more constituents of the catalyst's lattice is considered. It is known as the Mars van Krevelen (MVK) mechanism. This is applied by introducing two catalyst sites, namely catalyst support-based site-2, [V_2] and surface lattice oxygen in an oxidized site-1, [V_1^o]. The adsorbed propane reacts with the lattice oxygen in an oxidized site-1, [V_1^o] to give propylene. The lattice oxygen also react with adsorbed propane and adsorbed propylene product to give carbon oxides. Air is used to renegerate the catalyst by reacting reduced site-1 of the catalyst in excess air.

This is explained in a proposed mechanism highlighted below

Adsorption of Propane on a catalyst support-based site-2 [V_2] on the catalyst surface:

$$C_3H_{8\,(g)} + [V_2]_{(s)} \xleftrightarrow{K_1} C_3H_8\text{-}[V_2]_{s\,(s)} \quad (6.2)$$

Surface Reaction

$$C_3H_8\text{-}[V_2]_{s\,(s)} + 2\,[V_1^0]_s \xrightarrow{k_1} C_3H_6\text{-}[V_2]_s + H_2O_{(g)} + [V_1^0]_s + [V_1^R]_s \quad (6.3)$$

$$C_3H_8\text{-}[V_2]_s + (4+3x)\,[V_1^0]_s \xrightarrow{k_2} 3\,CO_{x(g)} + 4\,H_2O_{(g)} + [V_2]_s + (4+3x)[V_1^R]_s \quad (6.4)$$

$$C_3H_6\text{-}[V_2]_s + (3+3x)\,[V_1^0]_s \xrightarrow{k_3} 3\,CO_{x(g)} + 3\,H_2O_{(g)} + [V_2]_s + (3+3x)\,[V_1^R]_s \quad (6.5)$$

Desorption of Products

$$C_3H_6\text{-}[V_2]_s \xleftrightarrow{K_2} C_3H_6 + [V_2]_s \quad (6.6)$$

Regeneration of the reduced catalyst

$$O_{2(g)} + [V_1^R]_s \rightarrow [V_1^0]_s + [V_1^0]_s \quad (6.7)$$

According for the MVK mechanism, the reaction rates were formulated as follows:

$$r_1 = k_1\theta_{C_3H_8}(1-\alpha) \quad (6.8)$$

$$r_2 = k_2\theta_{C_3H_8}(1-\alpha) \quad (6.9)$$

$$r_3 = k_3\theta_{C_3H_6}(1-\alpha) \quad (6.10)$$

Where $\theta_{C_3H_8}$ and $\theta_{C_3H_6}$ are the surface coverage of adsorbed species of propane and propylene respectively.

r_1, r_2 and r_3 are the reaction rates of propane ODH, primary combustion of propane and secondary propylene product combustion. k1, k2 and k3 are the reaction rate constants of propane ODH, primary combustion of propane and secondary propylene product combustion.

$1-\alpha=\tau$ which represents the oxidized vanadium site or degree of oxidation of catalyst

The fractional coverage of propane and propylene can be expressed as follows

$$\theta_{C_3H_8} = \frac{K_1C_1}{1+K_1C_1+K_2C_2} \tag{6.11}$$

$$\theta_{C_3H_6} = \frac{K_2C_2}{1+K_1C_1+K_2C_2} \tag{6.12}$$

C_1 and C_2 are concentrations of propane and propylene respectively

The following assumptions were made in the mole balance of the propane ODH in CREC Riser Simulator:

(i) The oxidative dehydrogenation of propane is irreversible

(ii) The temperature change noticed during reaction runs is negligible, which signifies little influence of heat of reaction. This confirms the validity of assuming isothermal reaction conditions

(iii) All the reactions took place with a single function of deactivation

By substituting equations (11) and (12) into equations (8), (9) and (10), the following were obtained

$$r_1 = k_1.\frac{K_1C_1}{1+K_1C_1+K_2C_2}\ .e^{-\lambda(X_{C_3H_8})} \tag{6.13}$$

$$r_2 = k_2.\frac{K_1C_1}{1+K_1C_1+K_2C_2}\ .e^{-\lambda(X_{C_3H_8})} \tag{6.14}$$

$$r_3 = k_3 . \frac{K_2 C_2}{1+K_1 C_1+K_2 C_2} . e^{-\lambda(X_{C_3H_8})} \quad (6.15)$$

Based on the assumptions, three sets of differential equations can be obtain from the mole balance of three considered species

Rate of disappearance of propane

$$r_1 = -(r_1 + r_2) \quad (6.16)$$

Rate of formation of propylene

$$r_2 = (r_1 - r_3) \quad (6.17)$$

Rate of formation of CO_x

$$r_3 = (r_2 + r_3) \quad (6.18)$$

For a batch reactor

$$\frac{dN_i}{dt} = r_i V \quad (6.19)$$

$$\frac{1}{V}\frac{dN_i}{dt} = r_i \quad (6.20)$$

$$\frac{dC_i}{dt} = r_i \quad (6.21)$$

Since a catalytic reaction is considered, weight of catalyst, Wc and volume of reactor, Vr could be introduced into the above equation

$$r_i = \frac{V_r}{W_c}\frac{dC_i}{dt} \quad (6.22)$$

The concentration of any species can be treated as a function of its mass fraction

$$C_i = \frac{y_i W_1}{MW_i V_r} \quad (6.23)$$

$$dC_i = \frac{W_1}{MW_i V_r}\, dy_i \quad (6.24)$$

$$r_i = \frac{V_r}{W_c} . \frac{W_1}{MW_i V_r}\frac{dy_i}{dt} \quad (6.25)$$

Where W_1, y_1, y_2, y_3 are the mass of the propane feed, mass fraction of propane, propylene and carbon (IV) oxide respectively

$$\frac{dy_1}{dt} = \frac{MW_1W_c}{W_1}.\left[-(k_1+k_2).\frac{K_1C_1}{1+K_1C_1+K_2C_2}\ .e^{-\lambda(X_{C_3H_8})}\right] \tag{6.26}$$

$$\frac{dy_1}{dt} = \frac{MW_1W_c}{W_1}.\left[\frac{k_1K_1C_1-k_3K_2C_2}{1+K_1C_1+K_2C_2}\ .e^{-\lambda(X_{C_3H_8})}\right] \tag{6.27}$$

$$\frac{dy_{CO_x}}{dt} = \frac{MW_3W_c}{W_1}.\left[\frac{k_2K_1C_1+k_3K_2C_2}{1+K_1C_1+K_2C_2}\ .e^{-\lambda(X_{C_3H_8})}\right] \tag{6.28}$$

Taken $\beta = \frac{W_1}{MW_1V_r}$ (6.29)

$$\gamma = \frac{W_1}{MW_2V_r} \tag{6.30}$$

$$\delta = \frac{W_1}{MW_3V_r} \tag{6.31}$$

$$\frac{dy_1}{dt} = \frac{MW_1W_c}{W_1}.\left[-(k_1+k_2).\frac{K_1.\beta.y_1}{1+K_1.\beta.y_1+K_2.\gamma.y_2}\ .e^{-\lambda(X_{C_3H_8})}\right] \tag{6.32}$$

$$\frac{dy_2}{dt} = \frac{MW_2W_c}{W_1}.\left[\frac{k_1K_1.\beta.y_1-k_3.K_2.\gamma.y_2}{1+K_1.\beta.y_1+K_2.\gamma.y_2}\ .e^{-\lambda(X_{C_3H_8})}\right] \tag{6.33}$$

$$\frac{dy_3}{dt} = \frac{MW_3W_c}{W_1}.\left[\frac{k_2K_1.\beta.y_1+k_3K_2.\gamma.y_2}{1+K_1.\beta.y_1+K_2.\gamma.y_2}\ .e^{-\lambda(X_{C_3H_8})}\right] \tag{6.34}$$

The intrinsic rate constant can be evaluated from Arrhenius equation

$$k = k_o.e^{-\frac{E}{RT}} \tag{6.35}$$

k_o = Frequency factor or pre-exponential factor

k=reaction rate constant

Considering the centering temperature, an additional equation are obtained as shown below

$$k_c = k_o.e^{-\frac{E}{RT_c}} \tag{6.36}$$

Where k_c is the rate constant at centering temperature, T_c = centering temperature

Dividing the two equations, the equation below is obtained

$$\frac{k}{k_c} = e^{-\frac{E}{R}\left(\frac{1}{T}-\frac{1}{T_c}\right)} \tag{6.37}$$

$$k = k_c e^{-\frac{E}{R}\left(\frac{1}{T}-\frac{1}{T_c}\right)} \tag{6.38}$$

Adsorption equilibrium constant can also be obtained from the thermodynamic relations given below

$$K_i = e^{-\frac{\Delta H^o_{ads,i}}{RT}} \tag{6.39}$$

Considering the centering temperature in the above equation

$$K_i = K_{i_c} e^{-\frac{\Delta H^o_{ads,i}}{R}\left(\left(\frac{1}{T}-\frac{1}{T_c}\right)\right.} \tag{6.40}$$

6.4. Model Evaluation

Eleven parameters were used in the model equations. A nonlinear least square regression method was used to evaluate the optimum parameters that minimize the sum of square of the difference between the observed values of the reaction's mass fraction and the calculated values from the model.

$$\text{Minimum Sum of Square of Errors} = \sum_{i=1}^{n}(y_i^{obs} - y_i^{model})^2 \tag{6.41}$$

The three set of ordinary differential equations was solved using MATLAB function ''ode15s''

The criteria of optimization was done on the basis of the fact that there must be negative heat of adsorption and positive rate constants and activation energies of all the reactions.

The parameters are k_1^o, k_2^o, k_3^o, E_1, E_2, E_3, K_1^o, K_2^o, $-\Delta H_1$, $-\Delta H_2$ and λ

The mass fractions of propane, propylene and carbon (IV) oxide at 550 ^{o}C, 580 ^{o}C, 610 ^{o}C and 640 ^{o}C for each different reaction times (10 s, 17 s, 24 s and 31 s) were used for the evaluation of parameters. The specific rate constants was expressed using Arrhenius type of temperature- dependence function.

Table 6.1. Kinetic Parameters for the Proposed Kinetic Model

Parameter	VOx/CaO-γAl_2O_3 (1:4)	VOx/CaO-γAl_2O_3 (1:1)	VOx/CaO
	Values		
k_1^o (mol/gcat.s)	0.04056	0.1254	0.1044
k_2^o (mol/gcat.s)	0.04831	0.06691	0.08876
k_3^o (mol/gcat.s)	0.0006904	0.0017896	0.4402
E_1 (KJ/mol)	124.87	120.72	121.89
E_2 (KJ/mol)	52.85	52.65	32.26
E_3 (KJ/mol)	72.54	52.54	43.28
K_1^o (cm^3/mol)	8.672	8.313	8.857
K_2^o (cm^3/mol)	2.995	2.703	2.962
$-\Delta H_1$ (KJ/mol)	0.6818	0.6718	0.6806

$-\Delta H_2$ (KJ/mol)	0.5459	0.6164	0.6249
λ	0.0010	0.0011	0.0001

The data shows clearly the values of the specific rate constant of the ODH reaction, propane combustion and propylene combustion. The specific rate constant of the ODH reaction for VOx/CaO-γAl_2O_3 (1:1) catalyst is the highest as compared to the other two catalyst, while it is not the highest in the case of the propane and propylene combustion reaction. This shows that the VOx/CaO-γAl_2O_3 (1:1) catalyst give a better influence on the reaction rate as compared to the other two catalysts. This can be attributed to the moderate level of acidity of the VOx/CaO-γAl_2O_3 (1:1) catalyst.

The activation energy of the VOx/CaO-γAl_2O_3 (1:1) catalyst in the case of the ODH reaction have the lowest value. It means that the energy required before ODH reaction can take place is lowest for VOx/CaO-γAl_2O_3 (1:1) catalyst. The main function of a catalyst is to lower the activation energy of reaction. It means the VOx/CaO-γAl_2O_3 (1:1) catalyst did the best job as a result of it lowest activation for the ODH reaction.

The activation energies obtained for the ODH reaction is higher than that of the propane combustion and propylene combustion for all the three catalysts. The activation energies of ODH reaction is slightly higher than the sum of the activation energies of the two combustion reaction. This explain the limited values of propylene selectivity in oxidative dehydrogenation reaction.

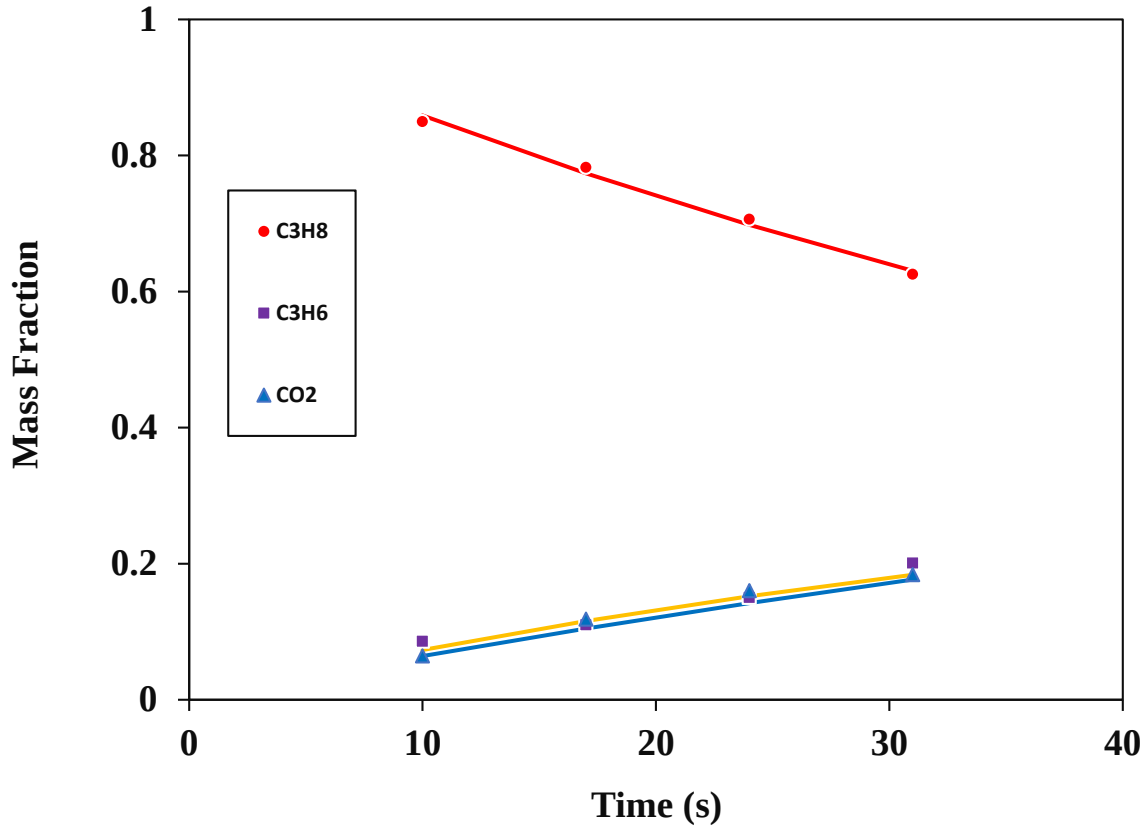

Fig. 6.2. Mass fraction of propane, propylene and carbon (IV) oxide from experimental data and modelled equation(-). Catalyst: VOx/CaO-γAl_2O_3 (1:4) and T: 640 ^oC

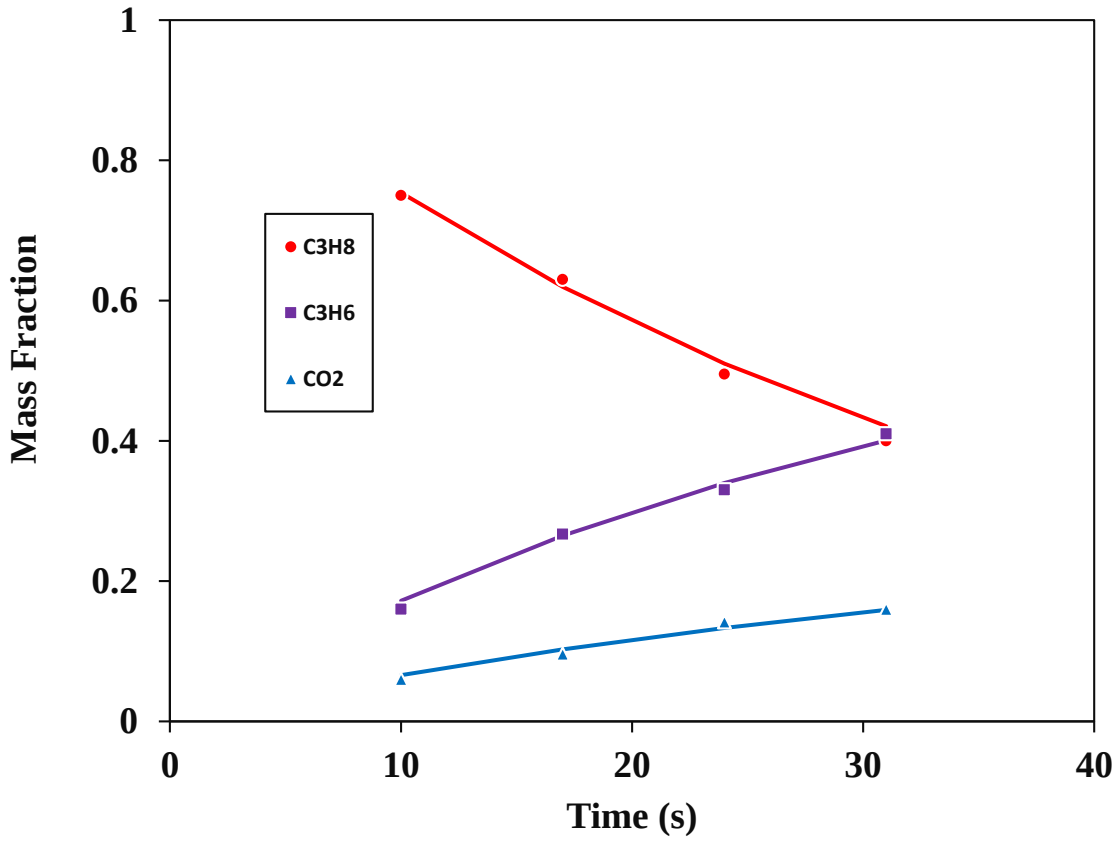

Fig. 6.3. Mass fractions of propane, propylene and carbon (IV) oxide from experimental data and modelled equation(-). Catalyst: VOx/CaO-γAl_2O_3 (1:1) and T: 640 ^oC

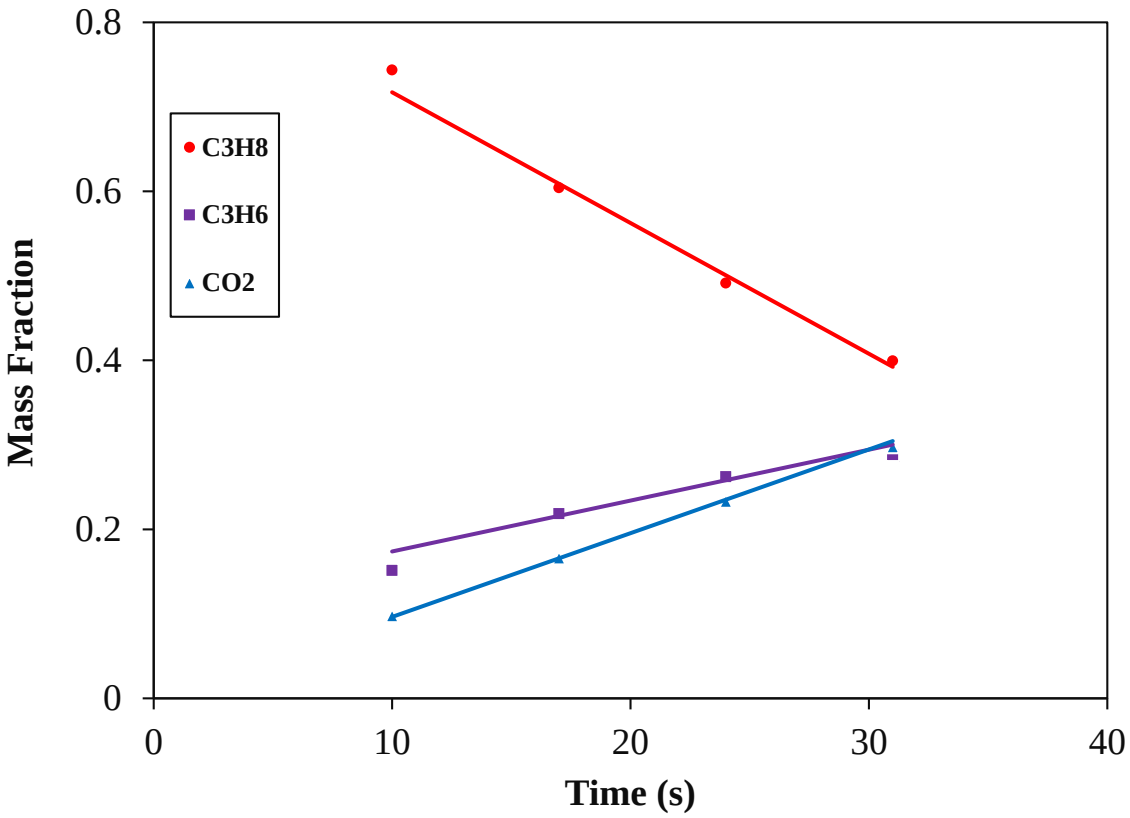

Fig. 6.4. Mass fractions of propane, propylene and carbon (IV) oxide from experimental data and modelled equation(-). Catalyst: VOx/CaO and T: 640 ^{o}C

CHAPTER 7

CONCLUSION AND RECOMMENDATION

7.1 Conclusions

The following are the conclusions of the present study:

i. FTIR, Raman and XRD analysis indicate the presence of V_2O_5, CaO and γAl_2O_3 in the synthesized catalyst.

ii. SEM images and elemental mapping shows good vanadium oxide dispersion on the mixed. CaO-γAl_2O_3 support.

iii. The repeated TPR/TPO experiments reveal that the synthesized catalysts are stable over repeated reduction and oxidation cycles.

iv. NH_3-TPD analysis shows that the increase of CaO loading decreased the acidity of the catalyst samples.

v. NH_3-TPD kinetics reveals decreased activation energy of desorption due to the increased amount of CaO in the catalyst sample, reflecting the increased metal-support interactions.

vi. Gas phase oxygen free conditions favors the formation of selective product propylene and minimizes the complete oxidations to CO_x. Higher degree of catalyst reductions gives more selective products.

vii. The catalyst with intermediate acidity and metal-support interaction (VO_x/CaO-γAl_2O_3 (1:1)) displays highest propylene selectivity (85 %) at higher propane conversion (65 %).

viii. A Langmuir-Hinshelwood type model fits the experimental ODH data adequately.

7.2 Recommendations

Based on the findings in this present work, the following are recommended for future research:

i. The science of the surface of VOx, γAl_2O_3 and CaO should be further examined in an effort to improve the conversion of propane

ii. Catalyst to feed ratio can used as variable alongside with temperature and time in order to obtain the ratio that will give the best result

References

[1] "Market Study: Propylene, Ceresana Research, February 2011." ceresana.com. Retrieved 2011-02-13.

[2] Ashford's Dictionary of Industrial Chemicals, Third Edition, 2011, ISBN 978-0-9522674-3-0, pages 7766-9.

[3] S.A. Al-Ghamdi (2013) oxygen-free propane oxidative dehydrogenation over vanadium oxide catalysts: reactivity and kinetic modeling. Ph.D dissertation monograph.

[4] E. Heracleous, M. Machli, A.A. Lemonidou, I.A. Vasalos, Oxidative dehydrogenation of dehydrogenation of ethane and propane over vanadia and molybdena supported catalysts, J. Mol. Catal. A: Chem. 232 (2005) 29–39.

[5] L. Chalakov, L.K. Rihko-Struckmann, B. Munder, K. Sundmacher, Oxidative dehydrogenation of ethane in an electrochemical packed-bed membrane reactor: Model and experimental validation, Chem. Eng. J. 145 (2009) 385-392.

[6] S.A. Al-Ghamdi, M. Volpe, M.M. Hossain, H.I. de Lasa, VO_x/c-Al_2O_3 catalyst for oxidative dehydrogenation of ethane to ethylene: desorption kinetics and catalytic activity. Appl. Catal. A: Gen. 450 (2013) 120–130.

[7] A.W.H. Elbadawi, M.S. Ba-Shammakh, S.A. Al-Ghamdi, S.A. Razzak, M.M. Hossain, Reduction kinetics and catalytic activity of VOx/γ-Al_2O_3-ZrO_2 for gas phase oxygen free ODH of ethane, Chem. Eng. J. 284 (2016) 448–457.

[8] I.A. Bakare, M. Shamseldin, S.A. Razzak, S.A. Al-Ghamdi, M.M. Hossain (2015), H.I. de Lasa, Fluidized bed ODH of ethane to ethylene over VO_x-MoO_x/γ-Al_2O_3 catalyst: Desorption kinetics and catalytic activity, Chem. Eng. J. 278 (2015) 207–216.

[9] M.M. Bhasin, Is true ethane oxydehydrogenation feasible, Top. Catal. 4 (2003) 145–149.

[10] L. Capek, R. Bulanek, J. Adam, L. Smolakova, H. Sheng-Yang, P. Cicmanec, Oxidative dehydrogenation of ethane over vanadium-based hexagonal mesoporous silica catalysts, Catal. Today 141 (2009) 282–287.

[11] L. Capek, J. Adam, T. Grygar, R. Bulanek, L. Vradman, G. Kosova-Kucerova, P.Cicmanec, P. Knotek, Oxidative dehydrogenation of ethane over vanadium supported on mesoporous materials of M41S family, Appl. Catal. A: Gen. 342 (2008) 99–106.

[12] F. Klose, T. Wolff, H. Lorenz, A. Seidelmorgenstern, Y. Suchorski, M. Piorkowska, H. Weiss, Active species on γ-alumina-supported vanadia catalysts: Nature and reducibility J. Catal. 247 (2007) 176–193.

[13] A. Klisinska, S. Loridant, B. Grzybowska, J. Stoch, I. Gressel, Effect of additives on properties of V_2O_5/SiO_2 and V_2O_5/MgO catalysts II. Structure and physicochemical properties of the catalysts and their correlations with oxidative dehydrogenation of propane and ethane, Appl. Catal. A: Gen. 309 (2006) 17–27.

[14] B. Grzybowska, A. Klisinska, K. Samson, I. Gressel, Effect of additives on properties of V_2O_5/SiO_2 and V_2O_5/MgO catalysts: I. Oxidative dehydrogenation of propane and ethane Appl. Catal. A: Gen. 309 (2006) 10–16.

[15] M.V. Martinez-Huerta, X. Gao, H. Tian, I.E. Wachs, J.L.G. Fierro, M.A. Banares, Oxidative dehydrogenation of ethane to ethylene over alumina-supported vanadium oxide catalysts: Relationship between molecular structures and chemical reactivity, Catal. Today 4 (2006) 279–287.

[16] R. Grabowski, J. Sloczynski, Kinetics of oxidative dehydrogenation of propane and ethane on VO_x/SiO_2 pure and with potassium additive, Chem. Eng. Process. 44 (2005) 1082–1093.

[17] E.P. Reddy, R.S. Varma, Preparation, characterization, and activity of Al_2O_3-supported V_2O_5 catalysts, J. Catal. 221 (2004) 93–101.

[18] F. Bozon-Verduraz, D.I. Enache, E. Bordes, A. Ensuque, Vanadium oxide catalysts supported on titania and zirconia: II. Selective oxidation of ethane to acetic acid and ethylene, Appl. Catal. A: Gen. 278 (2004) 103–110.

[19] D.I. Enache, E. Bordes, A. Ensuque, F. Bozon-Verduraz, Vanadium oxide catalysts supported on zirconia and titania: I. Preparation and characterization. Appl. Catal. A: Gen. 278 (2004) 93–102.

[20] P. Concepcion, M.T. Navarro, J.M. Lopez-Nieto, T. Blasco, B. Panzacchi, F. Rey, Vanadium oxide supported on mesoporous Al_2O_3: Preparation, characterization and reactivity, Catal. Today 96 (2004) 179–186.

[21] Z. Zhao, Y. Yamada, A. Ueda, H. Sakurai, T. Kobayashi, The roles of redox and acid–base properties of silica-supported vanadia catalysts in the selective oxidation of ethane, Catal. Today 95 (2004) 163–171.

[22] G. Busca, M. Panizza, C. Resini, F. Raccoli, R. Catani, S. Rossini, Oxidation of ethane over vanadia-alumina-based catalysts: co-feed and redox experiments, Chem. Eng. J. 93 (2003) 181–189.

[23] A.T. Bell, E. Iglesia, M.D. Argyle, K. Chen, Ethane Oxidative Dehydrogenation Pathways on Vanadium Oxide Catalysts, J. Phys. Chem. B 106 (2002) 5421–5427.

[24] H.I. de Lasa, M. Volpe, G. Tonetto, Butane dehydrogenation on vanadium supported catalysts under oxygen free atmosphere. Appl. Catal. A: Gen. 272 (2004) 69–78.

[25] A.T. Bell, A. Dinse, R. Schomacker, The role of lattice oxygen in the oxidative dehydrogenation of ethane on alumina-supported vanadium oxide, Phys. Chem. Chem. Phys. 29 (2009) 6119–6124.

[26] E.A. Mamedov, V.C. Corberfin, Oxidative dehydrogenation of lower alkanes on vanadium oxide-based catalysts. The present state of the art and outlooks. Appl. Catal. A: Gen. 127 (1995) 1–40.

[27] S.A. Al-Ghamdi, H.I. de Lasa, Propylene production via propane oxidative dehydrogenation over $VOx/\gamma Al_2O_3$ catalyst. Fuel 128 (2014) 120-140.

[28] A. Khodakov, B. Olthof, A.T. Bell, E. Iglesia, Structure and catalytic properties of supported vanadium oxides: support effects on oxidative dehydrogenation reactions. J. Catal. 181 (1999) 205–216.

[29] M.V. Martinez-Huerta, X. Gao, H. Tian, I.E. Wachs, J.L.G. Fierro, M.A. Banares, Oxidative dehydrogenation of ethane to ethylene over alumina-supported vanadium oxide catalysts: relationship between molecular structures and chemical reactivity. Catal. Today 118 (2006) 279–287.

[30] M.A. Banares, Supported metal oxide and other catalysts for ethane conversion: a review, Catal. Today 51 (1999) 319–348.

[31] I.E. Wachs, B.M. Weckhuysen, Structure and reactivity of surface vanadium oxide species on oxide supports, Appl. Catal. A: Gen. 157 (1997) 67–90.

[32] D.I. Enache, E. Bordes-Richard, F. Bozon-Verduraz, A. Ensuque, Vanadium oxide catalysts supported on zirconia and titania I. Preparation and characterization, Appl. Catal. A: Gen. 278 (2004) 93–102.

[33] J.M. Lopez-Nieto, J. Soler, P. Concepcion, J. Herguido, M. Menendez, J.Santamaria, Oxidative Dehydrogenation of Alkanes over V-based Catalysts: Influence of Redox Properties on Catalytic Performance, J. Catal. 185 (1999) 324–332.

[34] K. Chen, A.T. Bell, E. Iglesia, The relationship between the electronic and redox properties of dispersed metal oxides and their turnover rates in oxidative dehydrogenation reactions, J. Catal. 209 (2002) 35–42.

[35] F. Roozeboom, M.C. Mittelmeijer-Hazeleger, J.A. Moulijn, J. Medema, V.H.J. Beer De, P.J. Gellings, Vanadium oxide monolayer catalysts. 3. A Raman spectroscopic and temperature programmed reduction study of monolayer and crystal type vanadia on various supports, J. Phys. Chem. 84 (1980) 2783–2791.

[36] J.M. Lopez-Nieto, The selective oxidative activation of light alkanes from supported vanadia to multicomponent bulk V-containing catalysts. Top Catalysis 41 (2006) 3–15.

[37] G. Che-Galicia, R. Quintana-Solórzano, R.S. Ruiz-Martínez, J.S. Valente, C.O.C. Araiza, Kinetic modeling of the oxidative dehydrogenation of ethane to ethylene over a MoVTeNbO catalytic system, Chem. Eng. J. 252 (2014) 75-88.

[38] H. Kung, P.M. Michalakos, M.C. Kung, I. Jahan, Selectivity patterns in alkane oxidation over $Mg_3(VO_4)_2$–MgO, $Mg_2V_2O_7$, and $(VO)_2P_2O_7$. J. Catal. 140 (1993) 226–242.

[39] J. Santander, E. López, A. Diez, M. Dennehy, M. Pedernera, G. Tonetto, Ni–Nb mixed oxides: One-pot synthesis and catalytic activity for oxidative dehydrogenation of ethane, Chem. Eng. J. 255 (2014) 185-194.

[40] J.P. Bortolozzi, T. Weiss, L.B. Gutierrez, M.A. Ulla, Comparison of Ni and Ni–Ce/Al_2O_3 catalysts in granulated and structured forms: Their possible use in the oxidative dehydrogenation of ethane reaction, Chem. Eng. J. 246 (2014) 343–352.

[41] N.E. Quaranta, J. Soria, V. Cortés Corbéran, J.L.G. Fierro, Selective Oxidation of Ethanol to Acetaldehyde on $V_2O_5/TiO_2/SiO_2$ Catalysts J. Catal. 171 (1997) 1-13.

[42] Blekkan E.A, Andrey V. and Ilya Gorelkin (2012). Department of Chemical Engineering. Norwegian University of Science and Technology.

[43] Virgine Marie Therese Herauville(2012). Catalytic Dehydrogenation of Propane. Department of Chemical Engineering. Norwegian University of Science and Technology.

[44] Raquel Ramosl, M. Pilar Pinal, Miguel Men6ndez1, Jesk Santamarial and Gregory S. Patience. (2001). Oxidative Dehydrogenation of Propane to Propene: Kinetic Study on V/MgO. The Canadian Journal of Chemical Engineering. Volume 79.

[45] T. V. Malleswara Rao and Goutam Deo(2007). Kinetic Parameter Analysis for Propane ODH: V2O5/Al2O3 and MoO3/Al2O3 Catalysts. AIChE Journal Vol. 53, No. 6

[46] Ejiro Gbenedio, Zhentao Wu, Irfan Hatim, Benjamin F.K. Kingsbury, K. Li. A multifunctional Pd/alumina hollow fibre membrane reactor for propane dehydrogenation. Catalysis Today 156 (2010) 93–99.

[47] Baba Y. Jibril a, A.Y. Atta a, K. Melghit b, Z.M. El-Hadi b, Ala'a H. Al-Muhtaseb a. Performance of supported Mg0.15V2O5.152.4H2O nanowires in dehydrogenation of propane. Chemical Engineering Journal 193–194 (2012) 391–395.

[48] Yongzheng Duan, Yuming Zhou, Yiwei Zhang, Xiaoli Sheng, Shijian Zhou, Zewu Zhang. Effect of aluminum modification on catalytic properties of PtSn-based catalysts supported on SBA-15 for propane dehydrogenation. Journal of Natural Gas Chemistry 21(2012)207–214

[49] Raoul Naumann d'Alnoncourt. How to build a catalytic test reactor. Modern Methods in Heterogeneous Catalysis Research. WS 2010/2011

[50] Mengwei Xue, Yuming Zhou, Yiwei Zhang, XuanLiu, Yongzheng Duan, Xiaoli Sheng. Effect of cerium addition on catalytic performance of PtSnNa/ZSM-5 catalyst for propane dehydrogenation. Journal of Natural Gas Chemistry 21(2012)324–331.

[51] Yiwei Zhang, Yuming Zhou, Junjun Shi, Shijian Zhou, Xiaoli Sheng, Zewu Zhang, Sanming XiangComparative study of bimetallic Pt-Sn catalysts supported on different supports for propane dehydrogenation. Journal of Molecular Catalysis A: Chemical 381 (2014) 138– 147.

[52] Cavani F., Ballarini N., Cericola A. Oxidative dehydrogenation of ethane and propane: How far from commercial implementation? Catalysis Today 127 (2007) 113–131

[53] Sameer. A. Al-Ghamdi. (2013). Oxygen-Free Propane Oxidation Dehydogenation over Vanadium Oxide: Reactivity and Kinetic Modelling. PhD dissertation of the School of Graduate and Postdoctoral Studies. University of Western Ontario, London, Ontario.

[54] Bao Khanh Vua, Eun Woo Shina, Jeong-Myeong Hab, Seok Ki Kimb, Dong Jin Suhb, Won-Il Kimc, Hyoung-Lim Kohc, Young Gyo Choic, Seung-Bum Leed. The roles of $Ce_yZr_{1-y}O_2$ in propane dehydrogenation: Enhancing catalytic stability and decreasing coke combustion temperature. Applied Catalysis A: General 443– 444 (2012) 59– 66.

[55] Wua, Fei Heia, Nan Zhanga, Naijia Guana, Landong Lia, Wolfgang Grünertb, Oxidative dehydrogenation of propane with nitrous oxide overFe-ZSM-5 prepared by grafting: Characterization and performanceGuangjun. Applied Catalysis A: General 468 (2013) 230– 239.

[56] Yiwei Zhang, Yuming Zhou, Menghan Tang, Xuan Liu, Yongzheng Duan. Effect of La calcination temperature on catalytic performance of PtSnNaLa/ZSM-5 catalyst for propane dehydrogenation. Chemical Engineering Journal 181– 182 (2012) 530– 537.

[57] Farnaz Tahriri Zangeneh, Shokoufeh Mehrazma, Saeed Sahebdelfar. The influence of solvent on the performance of Pt–Sn/θ-Al2O3 propane dehydrogenation catalyst prepared by co-impregnation method. Fuel Processing Technology 109 (2013) 118–123.

[58] Yu Chang-lin, Xu Heng-yong, Chen Xi-rong, Ge Qing-jie, Wen-zhao. Preparation, characterization, and catalytic performance of PtZn-Sn/SBA-15 catalyst for propane dehydrogenation. Journal of Fuel Chemistry And Technology. Volume 38, Issue 3, June 2010.

[59] Changlin Yu, Hengyong Xu, Qingjie Ge, Wenzhao Li. Properties of the metallic phase of zinc-doped platinum catalysts for propane dehydrogenation. Journal of Molecular Catalysis A: Chemical 266 (2007) 80–87.

[60] Petr Sazama, Naveen K. Sathu, Edyta Tabor, Blanka Wichterlová, Šteˇpán Sklenák, Zdeneˇk Sobalík. Structure and critical function of Fe and acid sites in Fe-ZSM-5 in propane oxidative dehydrogenation with N2O and N2O decomposition. Journal of Catalysis 299 (2013) 188–203.

[61] Jia-Ling Wu, Miao Chen, Yong-Mei Liu, Yong Cao, He-Yong He , Kang-Nian Fan Sucrose-templated mesoporous β-Ga2O3 as a novel efficient catalyst for dehydrogenation of propane in the presence of CO_2. Catalysis Communications 30 (2013) 61–65.

[62] R. Molinder, T. P. Comyn, N. Hondow, J. E. Parkerc, V. Duponta, In situ X-ray diffraction of CaO based CO_2 sorbents, Energy Environ. Sci., 5 (2012) 8958-8969.

[63] A. Imtiaz, M.A. Farrukh, M. Khaleeq-ur-rahman, R. Adnan, Micelle-Assisted Synthesis of Al_2O_3·CaO Nanocatalyst: Optical Properties and Their Applications in Photodegradation of 2,4,6-Trinitrophenol, ScientificWorldJournal. 2013 (2013) 1-11.

[64] M. Sadeghi, M. H. Husseini, A Novel Method for the Synthesis of CaO Nanoparticle for the Decomposition of Sulfurous Pollutant, J. Appl. Chem. Res. 7 (2013) 39-49.

[65] X. Zhou, G. Wu, J. Wu, H. Yang, J. Wang and G. Gao, Carbon black anchored vanadium oxide nanobelts and their post-sintering counterpart (V_2O_5 nanobelts) as high performance cathode materials for lithium ion batteries, Phys. Chem. Chem. Phys, 16 (2014) 3973—3982.

[66] H. Bosc, J.K. Bert, J.G. Van Ommen, P.J. Gellings, Factors influencing the temperature programmed reduction profiles of vanadium pentoxide, J. Chem. Soc. Faraday Trans 80 (1984) 2479–2488.

[67] M.M, Koranne, J.G. Goodwin, G. Marcelin, Characterization of silica and alumina supported vanadia catalysts using temperature programmed reduction, J. Catal. 148 (1994) 369–377.

[68] S.A. Al-Ghamdi, M.M. Hossain, H.I. de Lasa, Kinetic modeling of ethane oxidative dehydrogenation over VOx/Al_2O_3 catalyst in a fluidized-bed riser simulator, Ind. Eng. Chem. Res. 52 (2013) 5235–5244.

[69] V. Balcaen, I. Sack, M. Olea, G.B. Marin, Transient kinetic modeling of the oxidative dehydrogenation of propane over a vanadia-based catalyst in the absence of O_2, Appl. Catal. A: Gen. 371 (2009) 31–42.

[70] O.S. Owen, M.C. Kung, H. Kung, The effect of oxide structure and cation reduction potential of vanadates on the selective oxidative dehydrogenation of butane and propane, Catal. Lett. 12 (1992) 45–50.

[71] Creaser D, Andersson B, Hudgins RR, Silverston PL, Transient kinetic analysis of the oxidative dehydrogenation of propane, J. Catal. 182 (1999) 264–269.

[72] V. Balcaen, I. Sack, M. Olea, G.B. Marin, Transient kinetic modeling of the oxidative dehydrogenation of propane over a vanadia-based catalyst in the absence of O_2, Appl. Catal. A Gen. 371 (2009) 31–42.

Vitae

Name	AYANDIRAN AFEES AYODEJI
Nationality	NIGERIAN
Date of Birth	5/5/1986
Email	g201303470@kfupm.edu.sa
Address	Room 204, Building 811, KFUPM, Saudi Arabia
Academic Background	B Eng Chemical Engineering
List of Publications:	Afees A. Ayandiran, Idris A. Bakare, Housam Binous, Sameer Al-Ghamdi, Shaikh A. Razzak, Mohammad M. Hossain. Oxidative dehydrogenation of propane over $VOx/CaO-\gamma Al_2O_3$ in gas phase oxygen free fluidized bed conditions. Submitted in Journal of Fuel.